Geochemistry Geophysics Geosystems G3
AN ELECTRONIC JOURNAL OF THE EARTH SCIENCES
Published by AGU and the Geochemical Society

Article
Volume 4, Number 2
18 February 2003
1017, doi:10.1029/2002GC000399
ISSN: 1525-2027

Buoyancy of the continental upper mantle

Robyn K. Kelly
Department of Geology and Geophysics, MIT-Woods Hole Oceanographic Institution Joint Program, Woods Hole, Massachusetts 02543, USA (rkelly@whoi.edu)

Peter B. Kelemen and Matthew Jull
Department of Geology and Geophysics, Woods Hole Oceanographic Institution, Woods Hole, Massachusetts 02543, USA

[1] The thermal boundary layer beneath continental cratons extends into the Earth's mantle to depths of at least 200 km. It has been proposed that chemical depletion of the lithospheric mantle during partial melting offsets the effect of increased density from conductive cooling, resulting in neutral buoyancy with respect to the underlying asthenosphere. Mineral compositions of garnet peridotite xenoliths in the Kaapvaal craton give equilibration temperatures and pressures that define a continental conductive geotherm intersecting a mantle adiabat with a potential temperature of 1300°C at ~60 kbar. We calculated normative densities for a "low-temperature" garnet and spinel peridotite xenolith suite using Mg#. At their temperatures and pressures of equilibration, all the low-temperature peridotites are positively buoyant with respect to the convecting mantle, which is inconsistent with the hypothesis of a neutrally buoyant thermal boundary layer. To account for the possibility that pressure, temperature, and mineral proportions may have varied over time, equilibrium solidus mineral assemblages for the low-temperature xenoliths over a range of pressures and temperatures were generated by free energy minimization using the program *Perplex* (http://www.perplex.ethz.ch). The equilibrium solidus densities for xenolith compositions along a 40 mW/m^2 conductive geotherm were compared with the density of pyrolite along a mantle adiabat with a potential temperature of 1300°C. These density calculations show that most of the xenoliths are positively buoyant with respect to asthenospheric mantle ("pyrolite") at their temperatures and pressures of equilibration, confirming the results from the normative density calculations. Also, at the onset of the accretion of the Kaapvaal craton, when the thermal boundary layer was thinner and hotter than today, these Kaapvaal peridotites would have been positively buoyant with respect to the convecting mantle at shallower pressures. Therefore we propose that peridotite at the base of the Kaapvaal "plate," in the mantle thermal boundary layer, was and is positively buoyant. Combined with evidence from the geoid and geomorphology, which suggests that cratons are isostatically compensated and neutrally buoyant, our results imply that there must be dense layers within cratonic crust or upper mantle that offset the positive buoyancy of depleted cratonic mantle peridotites.

Components: 9775 words, 14 figures.

Keywords: Kaapval craton; xenoliths; density; peridotites; buoyancy; mantle.

Index Terms: 1025 Geochemistry: Composition of the mantle; 8120 Tectonophysics: Dynamics of lithosphere and mantle—general; 3640 Mineralogy and Petrology: Igneous petrology; 8124 Tectonophysics: Earth's interior—composition and state (old 8105).

Received 21 June 2002; **Revised** 11 October 2002; **Accepted** 15 October 2002; **Published** 18 February 2003.

Kelly, R. K., P. B. Kelemen, and M. Jull, Buoyancy of the continental upper mantle, *Geochem. Geophys. Geosyst.*, *4*(2), 1017, doi:10.1029/2002GC000399, 2003.

1. Introduction

[2] Seismological and petrological studies have determined that beneath the continental cratons, the thermal boundary layer extends much deeper into the Earth's mantle than it does beneath younger continental and oceanic crust [*Jordan*, 1975a, 1975b]. Constraints from equilibration pressures and temperatures of mantle xenoliths erupted within cratons indicate a conductive thermal boundary layer thickness of about 180 to 240 km [e.g., *Finnerty and Boyd*, 1987; *Rudnick and Nyblade*, 1999; *Ryan et al.*, 1996; *Poudjom Djomani et al.*, 2001]. Teleseismic tomography has shown that this ''tectosphere'' [*Jordan*, 1975a] might locally extend to over 300 km depth [*Jordan*, 1988], an observation supported by the large flexural rigidities for old continental platforms [*Karner and Watts*, 1983; *Karner et al.*, 1983; *Kusznir and Karner*, 1985; *Forsyth*, 1985; *Lowry and Smith*, 1994; *Poudjom Djomani et al.*, 1995, 1999].

[3] If the thickness of the continental thermal boundary layer were not limited by small scale convective disruption at its base, and instead could continue thickening due to conductive cooling [e.g., *Parsons and Sclater*, 1977], the thermal boundary layer in the subcratonic mantle could conceivably achieve the depth that is inferred from seismic data beneath the cratons [*Jordan*, 1988]. However, there are indications that the cratonic thermal boundary layers do not develop due to conductive cooling alone [*Jordan*, 1988]. Though conductive cooling could explain the thickening of the lithosphere, it would also require subsidence of the surface to the point that the cratons should either be under water or should have overlying sedimentary layers more than ~5 km thick, neither of which is observed [*Jordan*, 1975a; *Oxburgh and Parmentier*, 1978; *Poupinet and de Voogd*, 1981]. Also, if the cratonic upper mantle were simply a thick thermal boundary layer with near-surface isostatic compensation, this shallow compensation would be reflected in the long-wavelength geoid. This compensation is not evident [*Jordan*, 1975a; *Haxby and Turcotte*, 1978; *Parsons and Richter*, 1980; *Richards and Hager*, 1984].

[4] Long-term conductive cooling will also result in the lithosphere becoming negatively buoyant with respect to the underlying convecting mantle. This negative buoyancy could create convective instability of the lithosphere, with all or part of the thermal boundary layer foundering into the convecting mantle [e.g., *Bird*, 1979; *Houseman et al.*, 1981]. The thickness and stability of the thermal boundary layer underneath cratons, as indicated seismically and based on xenolith studies, suggest that convective instabilities have not removed large parts of the cratonic upper mantle for several billion years [*Jordan*, 1975a; *Parsons and McKenzie*, 1978].

[5] To explain the formation and accretion of stable cratonic upper mantle, *Jordan* [1988] postulated the existence of a chemical boundary layer in the mantle beneath cratons that is sufficiently buoyant and viscous to be stabilized against convection. This chemical boundary layer is depleted in basaltic materials relative to the mantle beneath mid-ocean ridges, counteracting the effect of increased density due to conductive cooling. At a given temperature, peridotites with high Mg# (molar 100 * Mg/(Mg + Fe)) due to extraction of heavier basaltic components have a lower density than those with lower Mg# [*O'Hara*, 1975; *Boyd and McCallister*, 1976; *Green and Lieberman*, 1976; *Jordan*, 1979]. *Jordan* [1988] derived a relationship between whole rock Mg# and density normalized to a standard temperature and pressure (normative density) demonstrating how compositional changes affect the buoyancy of continental mantle material. According to this relationship, a one unit increase in the Mg# will counteract the negative buoyancy caused by a temperature decrease of ~200°C. The proposed chemical boundary layer would be composed of residual mantle peridotites whose depletion by partial melting resulted in higher Mg#s than in the mantle beneath younger continental regions and oceanic plates. *Jordan* [1988] hypothesized an ''isopycnic'' condition whereby the increased buoyancy caused by depletion exactly offsets the thermally induced density contrast between the relatively cold thermal boundary layer and the comparatively hot asthenospheric mantle, creating a neutrally buoyant chemical boundary layer (Figure 1).

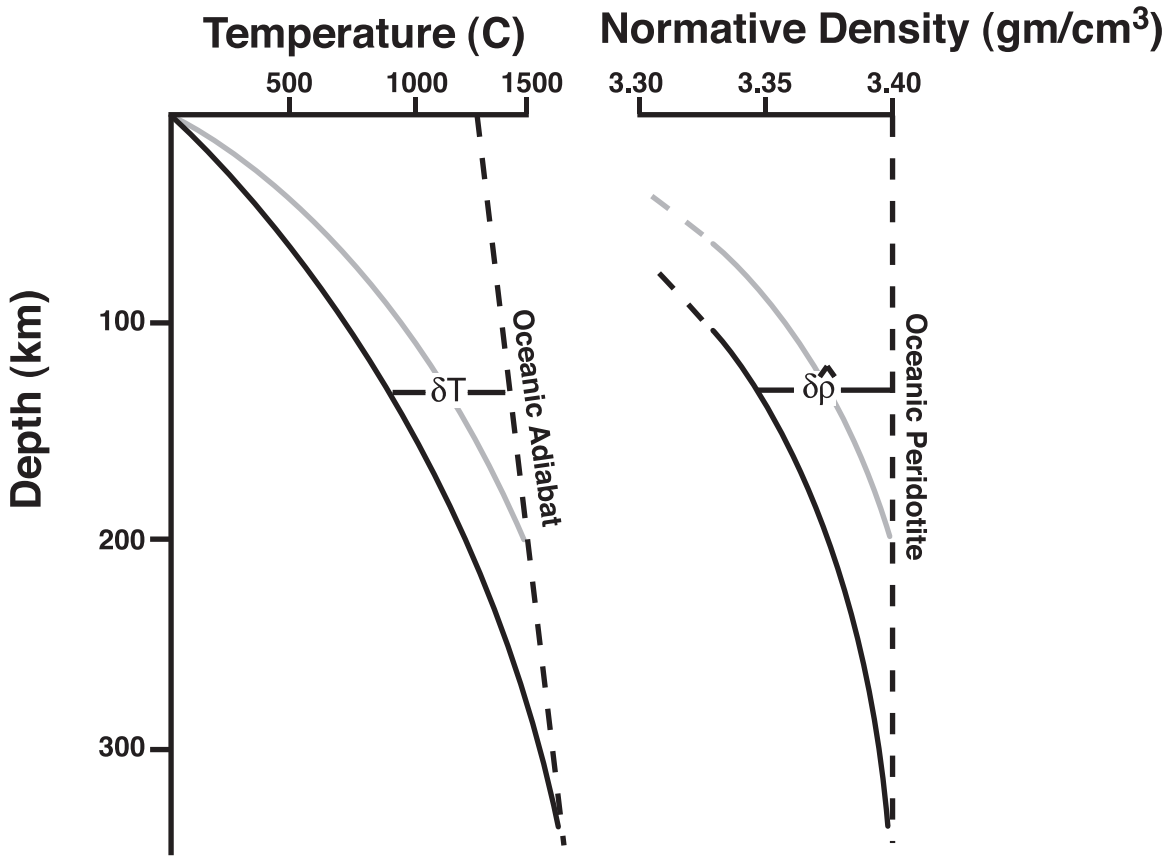

Figure 1. Illustration of the "isopycnic hypothesis" [*Jordan*, 1988], in which the cratonic upper mantle, extending to depths as great as 350 km, is neutrally buoyant with respect to the asthenosphere. The effect of low temperatures along a conductive geotherm is offset by chemical buoyancy, resulting from Fe extraction during large degrees of partial melting. Assuming that compressibilities and expansivities are the same for all mantle peridotites, a neutrally buoyant chemical boundary layer has a "normative density" at 1 bar and 25°C that offsets the density difference due to the temperature contrast between craton and asthenosphere at a given depth. Thus, for normative density $\hat{\rho}$, $\delta\hat{\rho}(z) = \hat{\rho}\alpha\ \delta T(z)$ (solid black line, calculated using $\alpha = 3 \times 10^{-5}$°C and an asthenospheric normative density of 3.4 gm/cm^3). If the thermal boundary layer is thinner, as suggested by thermobarometric data which indicate intersection of the cratonic geotherm and a mantle adiabat at about 200 km depth (solid gray line), then isopycnic densities must be higher at any given depth. Modified from *Jordan* [1988] by permission of the Oxford University Press.

[6] Building on the idea of a positively buoyant cratonic mantle [e.g., *Boyd and McCallister*, 1976], *Kelemen et al.* [1998] postulated that buoyant regions within the subcratonic lithospheric mantle form the thick thermal boundary observed beneath the cratons via tectonic thickening (via pure shear, imbrication, or compositional convection) of initially thin, neutrally buoyant, shallow mantle peridotite depleted by large degrees of decompression melting. Transport of shallow, high Mg# peridotite to greater depths and higher temperatures during thickening would produce a positive buoyancy contrast between the conductively cooling mantle lithosphere and the surrounding, convecting mantle. A stratified thermal boundary layer formed in this way, with a region of buoyant, residual peridotite near its base, would be more stable against convective instability than the neutrally buoyant mantle lithosphere proposed by *Jordan* [1988].

[7] Mantle xenoliths from cratonic regions provide the primary data on the chemical composition of the mantle near the base of the cratonic thermal boundary layer. The pressures and temperatures of

equilibration of these xenoliths, as well as their composition, vary from craton to craton. However, the xenolith suites from each craton exhibit similar characteristics. The Kaapvaal craton in South Africa, for example, has yielded suites of xenoliths that include both "high-temperature" xenoliths preserving equilibration pressures ranging from 55 kbar to 70 kbar (165–210 km), and "low-temperature" xenoliths with equilibration pressures less than 60 kbar (180 km) [e.g., *Finnerty and Boyd*, 1987]. These xenoliths include both garnet and spinel peridotites and have higher Mg#s than residual, oceanic peridotites dredged from the mid-ocean ridges ("abyssal peridotites"). This indicates the xenoliths have undergone higher degrees of melting at some point in their history [e.g., *Menzies*, 1990; *Boyd*, 1989]. Xenoliths from other cratons such as Siberia, central East Greenland, central West Greenland, and northern North America all have Mg#s comparable to Kaapvaal, pointing to similar degrees of melting [*Boyd et al.*, 1997; *Bernstein et al.*, 1998; *Mitchell*, 1977, 1978; *Eggler et al.*, 1987; *Larsen*, 1982; *Kopylova et al.*, 1998, 1999].

[8] Geothermobarometry together with density estimates for cratonic mantle xenolith compositions can be used to differentiate between the neutrally buoyant chemical boundary layer proposed by *Jordan* [1988] and the positively buoyant layer that *Kelemen et al.* [1998] proposed. *Boyd et al.* [1999] calculated the density of the Kaapvaal xenoliths at 1 bar and 25°C using the observed mode and mineral compositions. They found that along a continental geotherm that extends to 350 km depth, the shallow, low-temperature Kaapvaal peridotites are positively buoyant, while the deeper, high-temperature peridotites are negatively buoyant compared to "pyrolite" mantle [*Ringwood*, 1966] along an adiabat (Figure 2). These peridotite xenolith compositions do not fall along the isopycnic curve, yet - taken together - they might still form a neutrally buoyant thermal boundary layer. In contrast, for a continental geotherm that extends to 200 km, the majority of both the low- and high-temperature xenoliths are positively buoyant compared to pyrolite mantle along an adiabat (Figure 2). In this case, for the entire craton to be neutrally buoyant, the positive buoyancy of mantle peridotite (represented by the xenoliths) would have to be offset by the presence of high-density layers (e.g., eclogites) in the lower crust or upper mantle (Figure 3).

[9] Several recent studies support the result that the Archean cratonic mantle is positively buoyant due to depletion of basaltic components [*Griffin et al.*, 1998, 1999; *Lee and Rudnick*, 1999; *Lee et al.*, 2001; *Poudjom Djomani et al.*, 2001; *O'Reilly et al.*, 2001]. *Griffin et al.* [1998, 1999] determined an average bulk composition, modal assemblage, and density for the upper mantle at 1 bar and 20°C in Kaapvaal using garnet mineral concentrate data. *Poudjom Djomani et al.* [2001] calculated the density change with depth for this mean constant composition as a function of the thermal expansivity and bulk compressibility. They then integrated over depth to find the cumulative density of the subcratonic lithospheric mantle. In both cases, they found that the Archean cratonic thermal boundary layer is less dense than convecting asthenosphere below 60–100 km depth.

[10] These results may be consistent with the topography of the southern African plateau, more than 1 km above sea level, though most cratons average between 400 and 500 m in elevation [*Nyblade and Robinson*, 1994]. However, the anomalous elevation can also be modeled by invoking dynamic topography, where flow in the underlying mantle supports the excess topography [e.g., *Lithgow-Bertelloni and Gurnis*, 1997; *Lithgow-Bertelloni and Silver*, 1998]. The dynamic topography hypothesis may be consistent with the deep mantle low-velocity anomaly and long-wavelength geoid high beneath southern Africa [*Dziewonski*, 1984; *Richards and Hager*, 1984; *Hager et al.*, 1985; *Su et al.*, 1994; *Li and Romanowicz*, 1996; *Grand et al.*, 1997; *van der Hilst et al.*, 1997; *Lithgow-Bertelloni and Gurnis*, 1997; *Lithgow-Bertelloni and Silver*, 1998]. Additionally, other cratons that are as refractory as Kaapvaal (e.g., Greenland, Siberia, Superior) do not display the same elevation and geoid anomalies [*Dziewonski*, 1984; *Richards and Hager*, 1984; *Hager et al.*, 1985; *Su et al.*, 1994; *Li and Romanowicz*, 1996; *Grand et al.*, 1997; *van der Hilst et al.*, 1997; *Goes and*

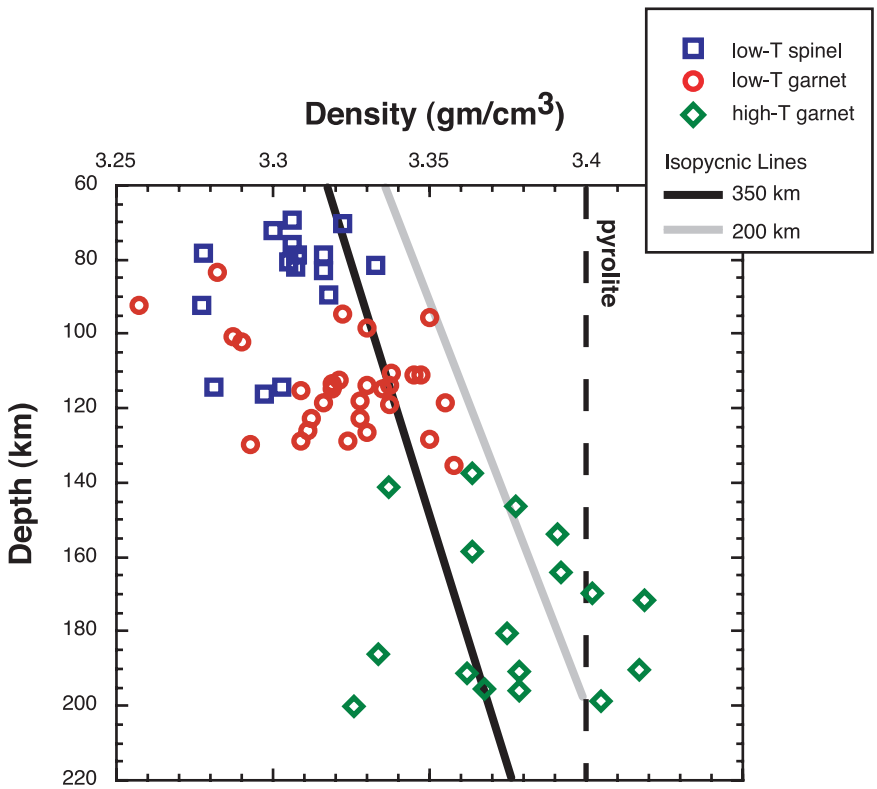

Figure 2. Densities for a suite of Kaapvaal garnet and spinel peridotite xenoliths at 1 bar and 25°C, calculated using the observed mode and mineral compositions, versus depth of equilibration, redrawn after *Boyd et al.* [1999] with addition of 200 km isopycnic curve. Open blue squares are spinel peridotites, open red circles are "low-temperature" garnet peridotites, and open green diamonds are "high-temperature" garnet peridotites. The dashed black line represents a pyrolite asthenosphere at a normative density of 3.4 gm/cm^3 [*Jordan*, 1988]. The black solid line represents the isopycnic condition for a thermal boundary layer that is 350 km thick [e.g., *Jordan*, 1988], and the gray solid line is the isopycnic condition for a thermal boundary layer that is 200 km thick [e.g., *Rudnick and Nyblade*, 1999]. Relative to the isopycnic curve for a 350 km thick thermal boundary layer, low-temperature Kaapvaal peridotites are more buoyant than convecting mantle with the composition of pyrolite, while deeper, high-temperature peridotites are denser than adiabatic mantle. However, for a thermal boundary layer only 200 km thick, almost all the Kaapvaal peridotites are more buoyant than the convecting mantle.

van der Lee, 2002]. For example, *Goes and van der Lee* [2002] estimated that the elevation of the Superior craton could be accounted for by depleted mantle with an average Mg#89–90 from the Moho to 250 km. A larger depletion over a smaller depth range could also explain the same topographic data. Average Mg#s of Archean cratonic xenoliths are in the range of 92–93 [*Boyd et al.*, 1997; *Bernstein et al.*, 1998; *Mitchell*, 1977, 1978; *Eggler et al.*, 1987; *Larsen*, 1982; *Kopylova et al.*, 1998, 1999].

[11] In order to place constraints on the lithospheric density structure beneath Archean cratons, we consider the possibility that the xenolith densities calculated by *Boyd et al.* [1999] at 1 bar and 25°C may not be representative of the density of these xenoliths at pressures and temperatures along a continental geotherm. For example, garnet is stable only at relatively high pressure, and at any pressure garnet proportions are smaller in Fe- and Al-poor depleted mantle compositions relative to fertile pyrolite. Using the same suite of low- and high-temperature Kaapvaal garnet and spinel peridotite xenoliths used by *Boyd et al.* [1999], we recalculated the pressure and temperature conditions of phase equilibration. In contrast to the *Griffin et al.* [1998, 1999] and *Poudjom Djomani et al.* [2001] methodology, we then used the bulk compositions of the peridotite xenoliths to calculate the equili-

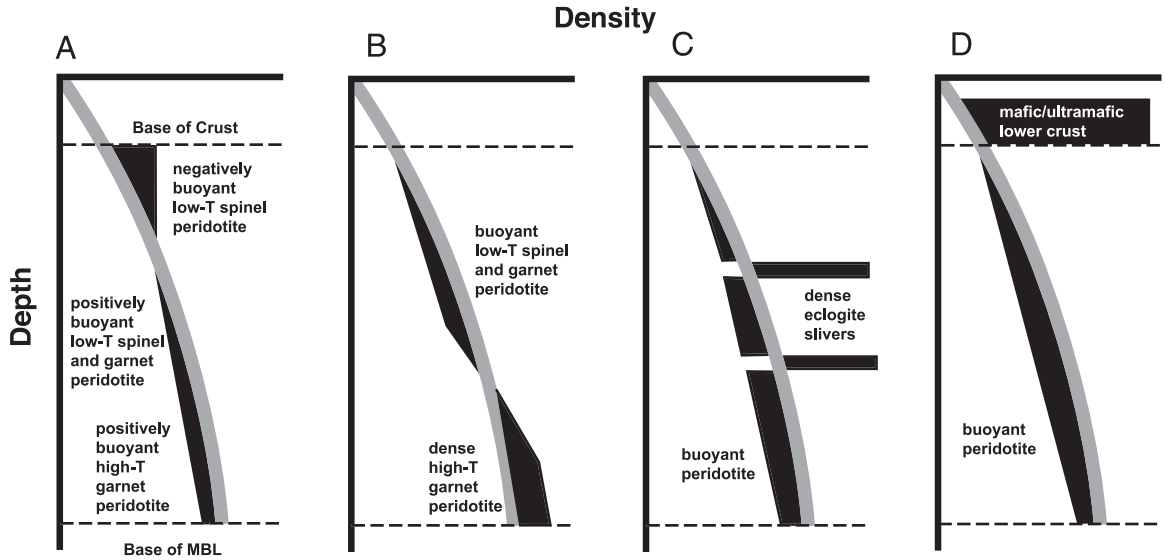

Figure 3. Possible density structures for a neutrally buoyant craton. The thermal boundary layer in the cratonic upper mantle could be neutrally buoyant if the density of the upper mantle fit an isopycnic condition at every depth (not shown). However, this is unlikely in detail and is not borne out by data. Alternatively, the cratonic mantle could be neutrally buoyant if (a) negatively buoyant, shallow peridotites were offset by positively buoyant, deeper peridotites, (b) shallow, highly depleted, positively buoyant material were offset by deeper, more Fe-rich, negatively buoyant material, or (c) positively buoyant, depleted peridotites were offset by layers of dense, basaltic rock in eclogite facies. (d) In addition, if the entire cratonic mantle is positively buoyant, this could still be offset by dense lower crust, for example by abundant garnet granulites near the base of the crust, to produce an isostatic cratonic section.

brium phase proportions over a range of pressures and temperatures, allowing us to determine the densities of the xenoliths over this range and not just at the pressure and temperature of equilibration. By doing so, we are able to assess the possible importance of varying phase proportions on density of these xenoliths and thus predict the density structure of the lithospheric mantle. Also, to make these calculations we used an internally consistent thermodynamic data set [*Holland and Powell*, 1998], which accounts for possible compositional effects on compressibility and expansivity.

2. Methodology

[12] Bulk rock compositions, modal assemblages, and mineral compositions for a large suite of garnet and spinel peridotite xenoliths from Kaapvaal were provided by F.R. Boyd. Pressures and temperatures of equilibration for the low- and high-temperature garnet peridotites were calculated using a two-pyroxene thermometer and Al-in-opx/garnet barometer, as discussed by *Brey and Kohler* [1990]. For the spinel peridotites, only temperatures of equilibration could be calculated, using a thermometer based on Al-Cr exchange between orthopyroxene and spinel [*Witt-Eickschen and Seck*, 1991]. Pressures of equilibration for the spinel peridotites were determined by interpolation along a 40 mW/m^2 continental geotherm [*Pollack and Chapman*, 1977] using the calculated temperatures.

[13] Densities were calculated using two different methods. The first method was a normative density ($\hat{\rho}$) calculation (density normalized to 1 bar and 25°C) using *Jordan*'s [1988] empirical relationship between whole rock Mg# and normative density:

$$\hat{\rho} = [5.093 - 0.0191 * 100 * \mathrm{Mg}/(\mathrm{Mg} + \mathrm{Fe})] \cdot \mathrm{gm/cm^3} \quad (1)$$

The second method utilized a subsolidus phase equilibrium calculation program called *Perplex* [*Connolly*, 1990] that uses thermodynamic data (in our case, *Holland and Powell* [1998]) to calculate the equilibrium phase assemblage at a given pressure and temperature based on the principle of free energy minimization in a multi-

component system. Densities were then calculated from the resulting equilibrium mineral assemblage, together with data on the compressibility and thermal expansion of minerals. These densities were compared to densities calculated in the same manner for a pyrolite mantle composition along an adiabatic geotherm with a potential temperature of 1300°C. (Using a potential temperature of 1350°C would not make a significant difference to our results; for example, this lowers the calculated density for pyrolite on an adiabat by ~0.001 gm/cm^3). This method is potentially better than the normative density approach [*Jordan*, 1988] and an empirical approach based on calculating densities at P and T from observed mineral proportions and compilations of mineral compressibility and expansivity [*Boyd and McCallister*, 1976; *Jordan*, 1979; *Griffin et al.*, 1998, 1999; *Boyd et al.*, 1999; *Lee et al.*, 2001; *Poudjom Djomani et al.*, 2001], because it provides a thermodynamically self-consistent result that includes variations in phase proportions as a function of temperature and pressure, and compositional effects on mineral compressibility and expansivity. In practice, we do not predict dramatic variations in phase proportions once peridotites are in the garnet stability field, and the method we have used involves several approximations, as discussed in section 3.2, so we view our results as complementary to the normative density and empirical approaches.

3. Results

3.1. Calculated Geotherms for Kaapvaal Garnet and Spinel Mantle Peridotites

[14] Geothermobarometry calculations were performed on three suites of mantle peridotite xenoliths from the Kaapvaal craton (22 low-temperature garnet/spinel-bearing peridotites, 18 low-temperature spinel-only peridotites, and 19 high-temperature garnet-bearing peridotites). The equilibration pressures and temperatures for the garnet-bearing mantle xenoliths are shown in Figure 4. Estimated equilibration conditions for the garnet peridotites differ slightly from those of *Boyd et al.* [1999], because they used a Ca-in-opx thermometer together with the *Brey and Kohler* [1990] opx/garnet barometer, whereas we used the two-pyroxene thermometer and the opx/garnet barometer from *Brey and Kohler* [1990]. Our calculations yield slightly higher equilibration temperatures and pressures compared to *Boyd et al.* [1999], but these differences do not significantly affect any of the results reported in this paper.

[15] Many of the low- and, especially, the high-temperature garnet peridotites have equilibration temperatures that are slightly hotter than those along the 40 mW/m^2 geotherm. *Rudnick and Nyblade* [1999] projected different model geotherms through suites of African peridotite thermobarometric data and found that 47 ± 2 mW/m^2 seemed to provide the best fit for the data. However, the high-temperature xenoliths preserve disequilibrium textures and zoning within minerals, so they may not record temperatures along a steady state geotherm. Throughout this paper, we used a 40 mW/m^2 geotherm to calculate the equilibration pressures for spinel peridotites, and the densities of all the xenoliths, with the expectation that this procedure will yield maximum density estimates.

3.2. Phase Assemblage and Density Variation From Bulk Rock Compositions

[16] *Perplex* is a series of programs (http://www.perplex.ethz.ch) that take a bulk rock chemical analysis and calculate the equilibrium subsolidus mineral assemblage at a given temperature and pressure using the principle of free energy minimization (see *Connolly* [1990] for details on method) and incorporating the most up-to-date, self-consistent thermodynamic data available [e.g., *Holland and Powell*, 1998]. Determination of the equilibrium mineral assemblage at a designated temperature and pressure allows the density of the sample to be calculated. In our calculations, below 800°C, the modal assemblages were held constant, as reaction rates are considered to be too slow to further modify phase proportions [e.g., *Hacker*, 1996]. Thus, below 800°C, the mineral assemblage at 800°C and the same pressure is used for density calculations, together with compressibilities and expansivities for that phase assemblage. Because the solid solution models for minerals in *Perplex* do not account well for the distribution of

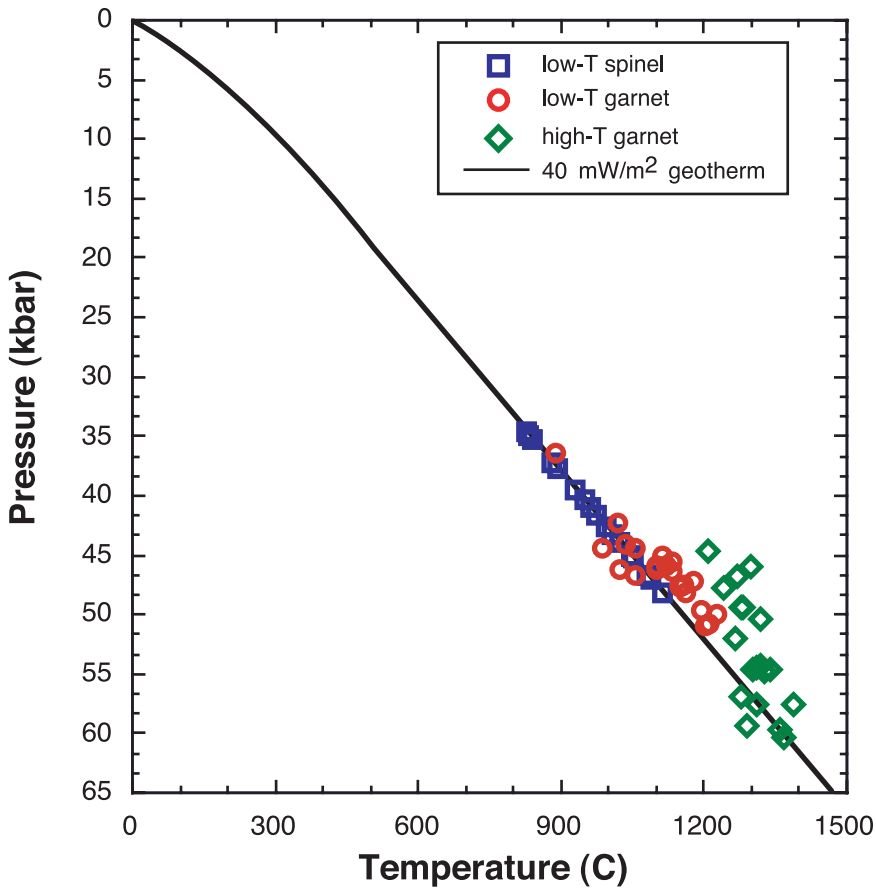

Figure 4. Estimated equilibration conditions for a suite of Kaapvaal spinel and garnet mantle peridotite xenoliths, compared to a 40 mW/m^2 conductive geotherm [*Pollack and Chapman*, 1977]. The open blue squares denote spinel-only peridotites. The open red circles represent low-temperature garnet-bearing peridotites. The open green diamonds are high-temperature garnet peridotites. Equilibration pressures and temperatures of the garnet-bearing peridotites were calculated using a two-pyroxene geothermometer and an Al-in-opx/garnet geobarometer [*Brey and Kohler*, 1990]. These define a conductive geotherm close to the 40 mW/m^2 geotherm, although they are also consistent with a hotter geotherm as proposed by *Rudnick and Nyblade* [1999]. For spinel-only peridotites, equilibration temperatures were calculated using a Cr- and Al-in-opx/spinel thermometer [*Witt-Eickschen and Seck*, 1991], and the equilibration pressures were interpolated from a 40 mW/m^2 conductive geotherm using the equilibration temperatures. Using these estimated pressures, the majority of the spinel peridotites are inferred to have equilibrated at lower pressures than the garnet-bearing peridotites.

Ti, Cr, Mn, K, and P, in this paper concentrations of six components were specified when calculating the equilibrium phase assemblage: SiO_2, Al_2O_3, FeO, MgO, CaO, and Na_2O. Comparisons of the calculated mineral modes for each bulk rock composition to the observed modes of each low-temperature peridotite at the respective pressure and temperature of equilibration are shown in Figure 5.

[17] Figure 6 provides a specific example of the calculated phase assemblages for spinel peridotite FRB 1382 and garnet peridotite PHN 4274 over a range of temperatures and pressures. As in the examples illustrated, none of the spinel peridotites formed spinel at their equilibrium conditions; instead, all formed garnet. Solid solutions in *Perplex* do not include Cr in any phase. The effect of Cr in natural systems is to stabilize spinel in peridotites, leading to the appearance of garnet and the disappearance of spinel at higher pressures than in a Cr-free system. *Perplex* also tended to overpredict the proportion of olivine while underpredicting the

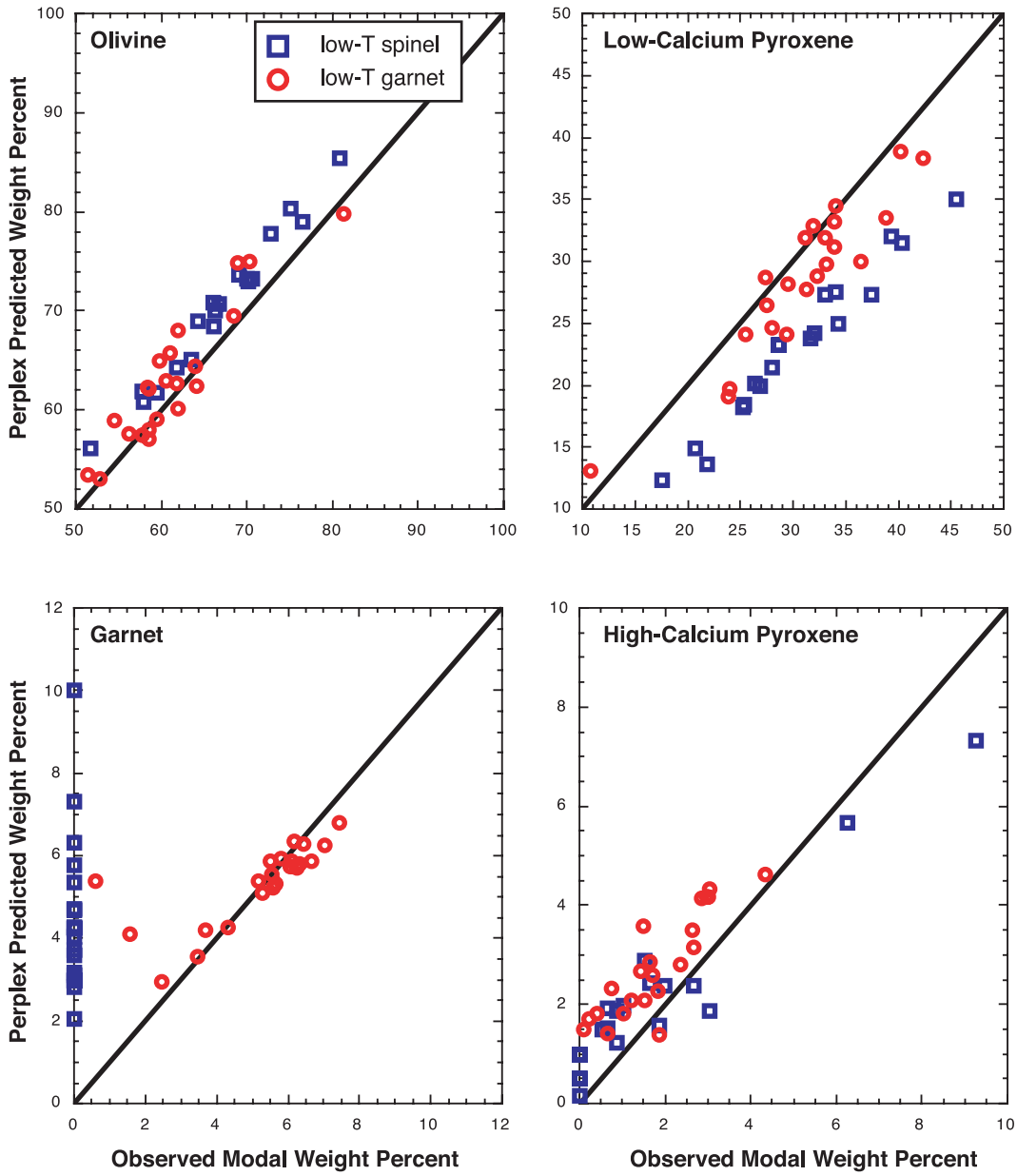

Figure 5. Comparison of calculated phase assemblages at the pressure and temperature of equilibration to observed phase assemblages for the low-temperature peridotites. The program *Perplex* was used to calculate phase assemblages from the bulk composition [*Connolly*, 1990]. Agreement between calculated and observed phase proportions is good, particularly for the garnet-bearing xenoliths. Calculated modes for spinel peridotites have garnet and no spinel at their equilibrium conditions. In addition, the calculated modes overpredict olivine and underpredict enstatite. This is most likely due, at least in part, to the presence of Cr_2O_3 in the spinel peridotites. *Perplex* does not account for Cr_2O_3 in peridotites, the presence of which enhances spinel stability and suppresses garnet formation.

proportion of enstatite for the spinel peridotites (Figure 5). This is related to the overabundance of garnet and the lack of spinel in the predicted phase assemblages, via the general reaction pyroxene + spinel = garnet + olivine. We can estimate the effect of the overprediction of garnet + olivine proportions on peridotite density using end-member data at 1 bar and 25°C for pyrope, almandine, uvarovite, grossular, spinel, hercynite, enstatite, ferrosilite, forsterite and fayalite from *Bass* [1995], and assuming ideal

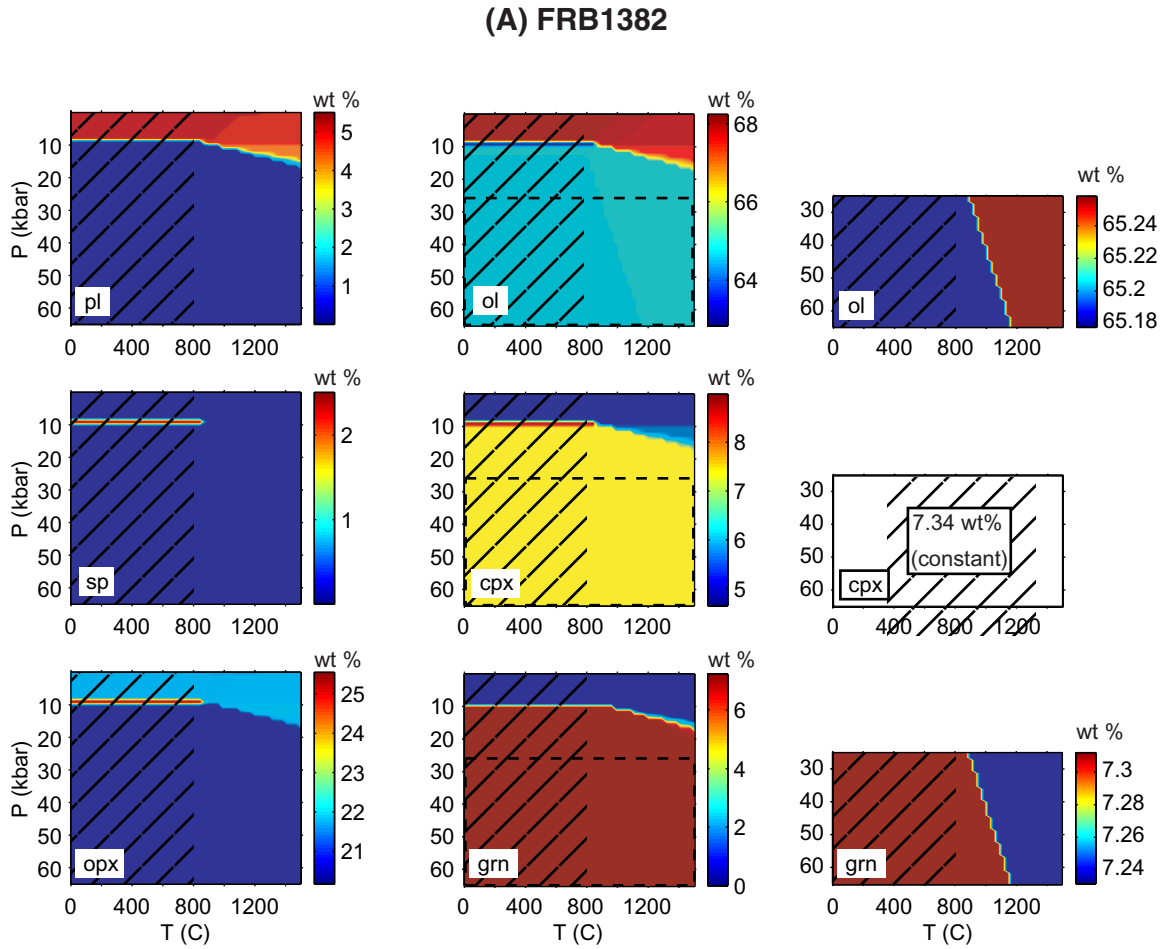

Figure 6. An example of the phase assemblages for (a) spinel peridotite FRB 1382 (Mg# 92.0) and (b) garnet peridotite PHN 4274 (Mg# 93.2) calculated over a range of temperatures and pressures using *Perplex*. Detailed panels on the right-hand side of Figures 6a and 6b (regions indicated by dashed borders) illustrate that formation of Al-rich pyroxene and Fe/Mg exchange between garnet and olivine do not have a large effect on the mineral proportions and density of the calculated phase assemblage. Diagonal lines indicate that the modal assemblages were held constant below 800°C.

mixing to estimate the density of MgCr and FeCr garnets. For the reactions

$$2Mg_2Si_2O_6 + MgAl_2O_4 = Mg_3Al_2Si_3O_{12} + Mg_2SiO_4,$$

$$2Fe_2Si_2O_6 + FeAl_2O_4 = Fe_3Al_2Si_3O_{12} + Fe_2SiO_4,$$

$$2Mg_2Si_2O_6 + MgCr_2O_4 = Mg_3Cr_2Si_3O_{12} + Mg_2SiO_4,$$

$$2Fe_2Si_2O_6 + FeCr_2O_4 = Fe_3Cr_2Si_3O_{12} + Fe_2SiO_4,$$

density changes at 1 bar and 25°C calculated in this way are +0.173, +0.265, +0.089, and +0.190 gm/cm^3, respectively. Since the garnet + olivine products for all of these reactions are denser than the pyroxene + spinel reactants, it is apparent that our calculated densities for Cr-free bulk compositions using *Perplex* are upper limits on the actual density of the peridotite assemblages at a given pressure and temperature. In this paper, we emphasize that our calculated densities are lower than those inferred from the isopycnic hypothesis. We suggest that most cratonic upper mantle peridotites are buoyant with respect to the convecting mantle. As a result, it is appropriate that our calculated densities are upper bounds for relatively Cr-rich cratonic peridotites.

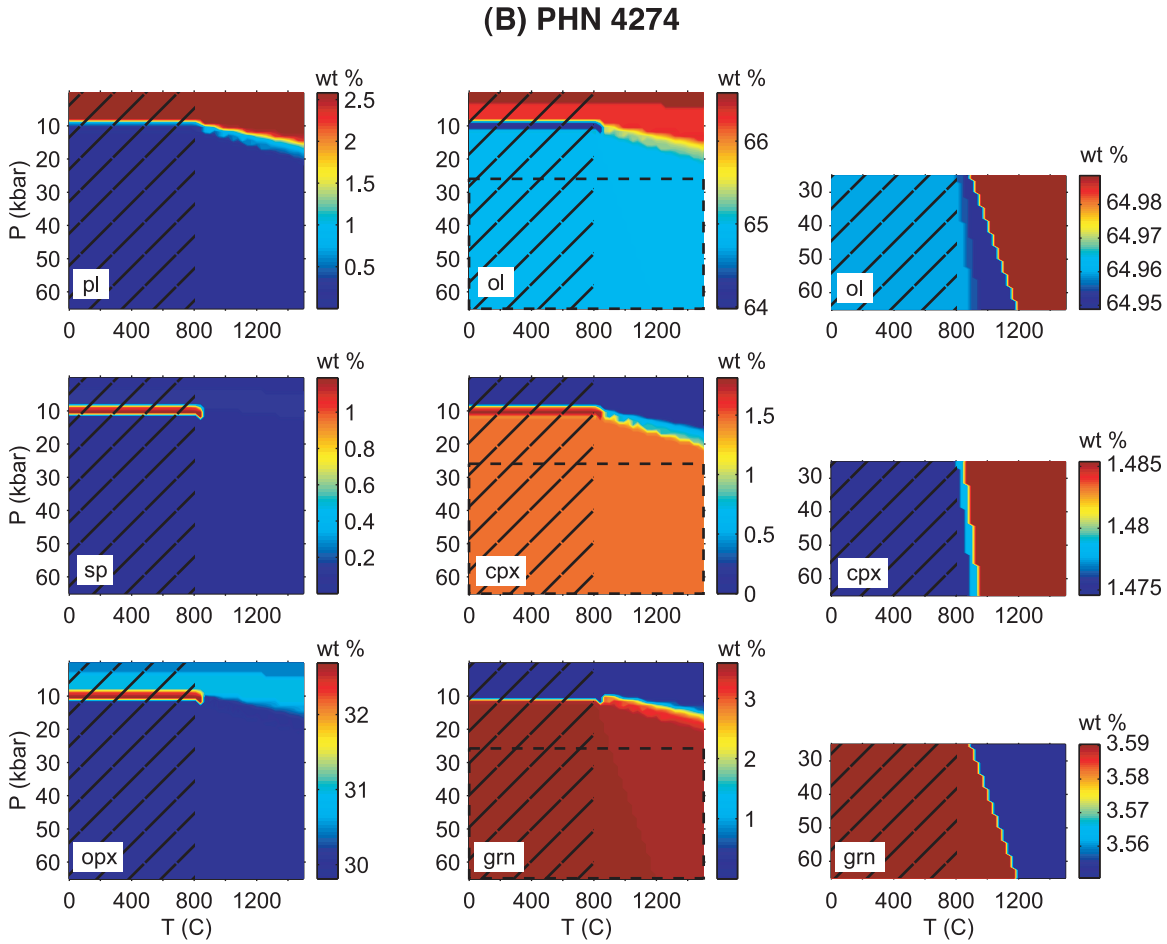

Figure 6. (continued)

[18] Figure 6 also shows three different types of reactions involving garnet formation and breakdown. The first type, associated with an abrupt increase in density over a narrow pressure interval, are familiar reactions at the low-pressure bound of the garnet lherzolite facies: pyroxene + spinel = garnet + olivine, and olivine + plagioclase = garnet ± jadeite-rich pyroxene. The others are reactions within the garnet lherzolite stability field that involve high-temperature formation of Al-rich pyroxene at the expense of garnet via reactions of the type

$$Mg_3Al_2Si_3O_{12} = MgAl_2SiO_6 + Mg_2Si_2O_6,$$

and Fe/Mg exchange between garnet and olivine, decreasing the weight proportion of garnet and increasing the weight proportion of olivine at high temperature via

$$Fe_3Al_2Si_3O_{12} + Mg_2SiO_4 = Mg_3Al_2Si_3O_{12} + Fe_2SiO_4.$$

[19] The effect of these reactions is illustrated in the detailed panels on the right-hand side of Figures 6a and 6b (regions indicated by dashed borders). As can be seen, we found that formation of Al-rich pyroxene and Fe/Mg exchange between garnet and olivine do not have a large effect on the mineral proportions and density of the calculated phase assemblage.

[20] The calculated densities at the equilibration pressures on the 40 mW/m^2 geotherm are compared to the calculated densities at the equilibration pressures and the equilibration temperatures for

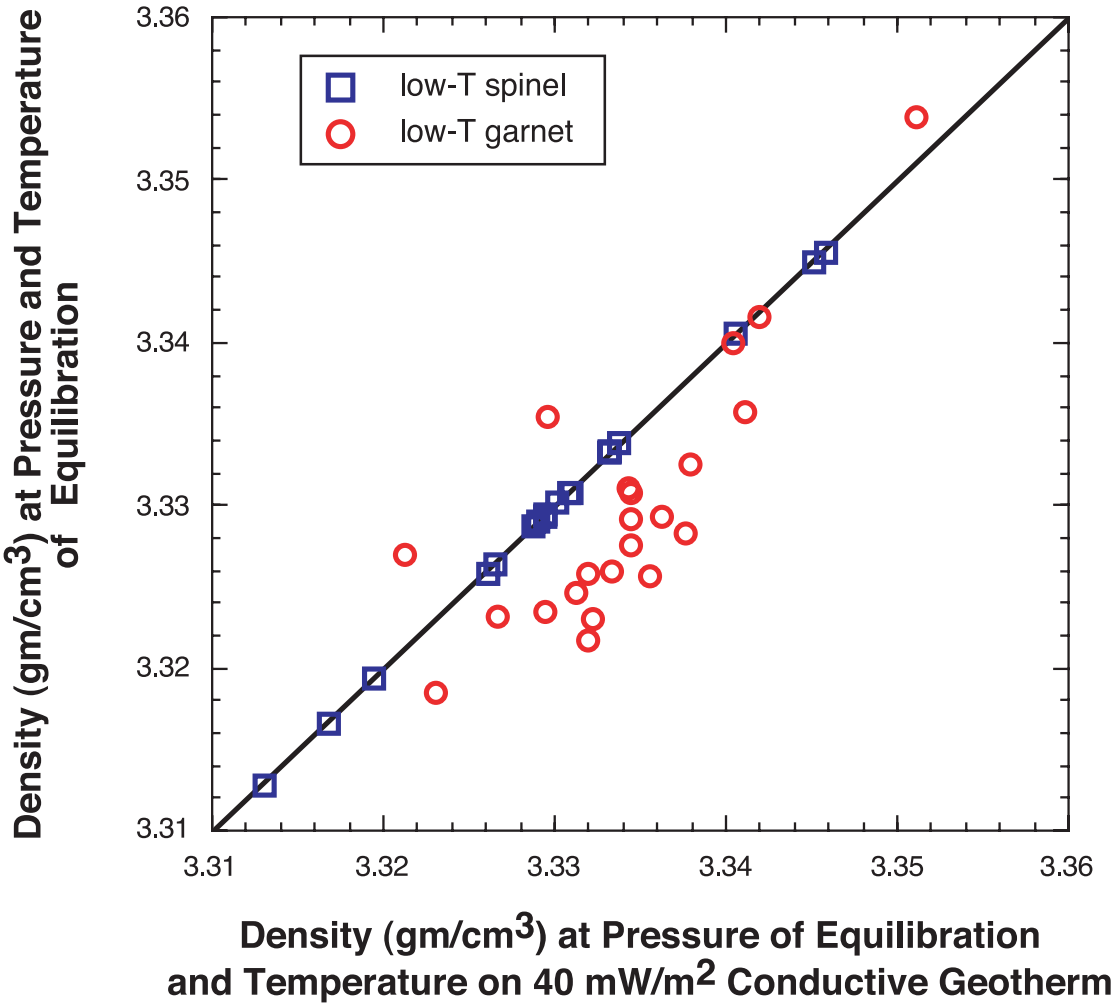

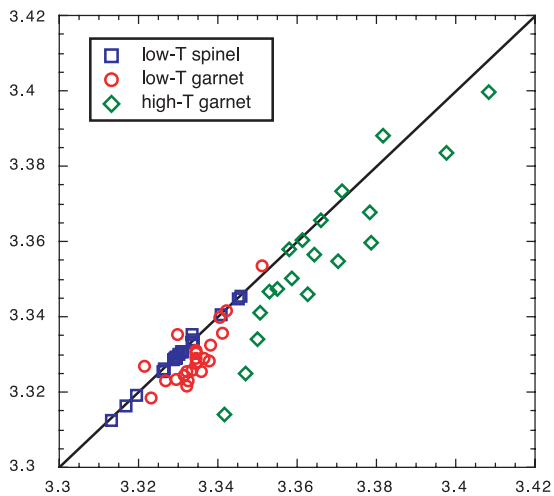

Figure 7. Comparison of densities calculated at equilibration temperatures with densities calculated at temperatures along a 40 mW/m^2 conductive geotherm; equilibration pressures were used for both density calculations. Low-temperature spinel and garnet peridotites are indicated with blue squares and red circles, respectively. The inset also includes high-temperature garnet peridotites in green diamonds. As discussed in the text, using equilibration pressures together with temperatures along a 40 mW/m^2 conductive geotherm provides higher density estimates for the bulk rock compositions, compared with density estimates using equilibration pressures and equilibration temperatures.

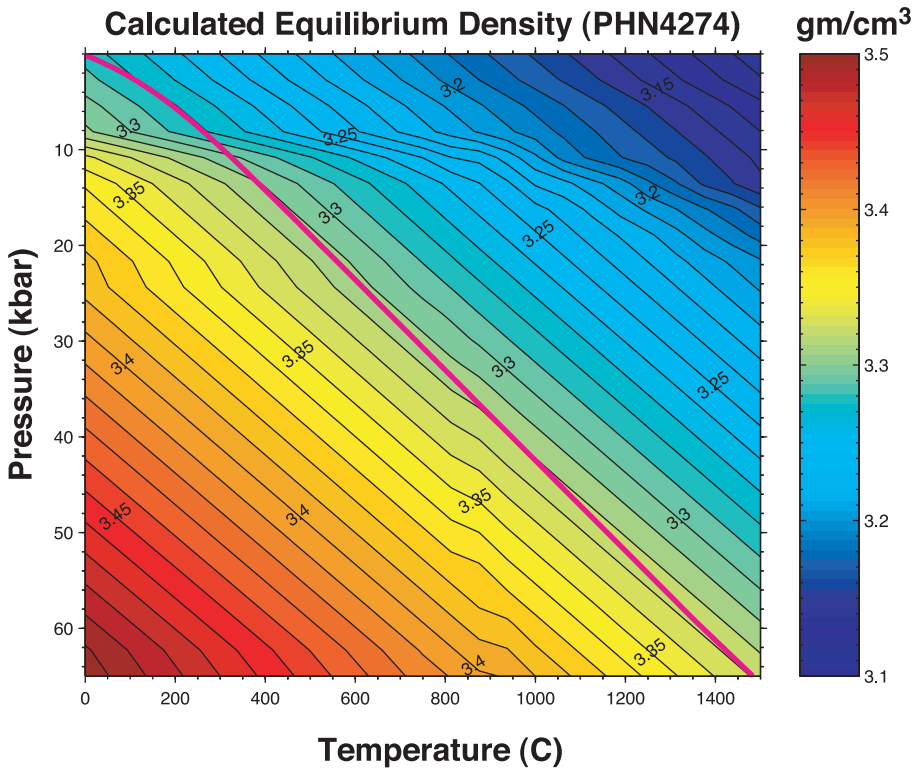

Figure 8. Contours of equilibrium density calculated using *Perplex* for low-temperature, garnet-bearing peridotite PHN 4274 (Mg# 93.2) from 0–65 kbar and 0–1500°C. The magenta line represents a 40 mW/m^2 conductive geotherm.

all samples in Figure 7. For most of the garnet peridotites, densities along the 40 mW/m^2 geotherm are higher than densities at the same depth and the equilibration temperature. Thus, the densities along the 40 mW/m^2 geotherm are upper-bound estimates of the actual densities of mantle peridotites along the Kaapvaal geotherm. As we pointed out in the previous paragraph, because we emphasize in this paper how low our calculated densities are compared to the convecting mantle, it is appropriate that we use upper-bound estimates for the calculated densities of cratonic peridotites.

[21] Pyrolite [*Ringwood*, 1966] was chosen as a reference mantle composition for comparison with the Kaapvaal mantle peridotite xenoliths. For the pyrolite composition and each of the garnet and spinel peridotites from Kaapvaal, equilibrium density grids for a temperature range of 0–1500°C and a pressure range of 0–65 kbar were calculated. Figure 8 is a contoured equilibrium density grid for garnet peridotite xenolith PHN 4274. A 40 mW/m^2 conductive geotherm is shown in magenta. For this particular sample, the conductive geotherm generally falls between the 3.31 gm/cm^3 and 3.33 gm/cm^3 contour lines. The equilibrium density grid for pyrolite is shown in Figure 9 with both the conductive geotherm and the adiabat with a potential temperature of 1300°C. The adiabat intersects the conductive geotherm at ~60 kbar where pyrolite has a calculated equilibrium density of 3.388 gm/cm^3.

[22] The normative densities [*Jordan*, 1988] and the *Perplex*-calculated equilibrium densities of the Kaapvaal garnet and spinel mantle peridotite xenoliths are plotted against pressure in Figure 10, using the equilibration pressures for the garnet peridotites and the inferred pressures for the spinel peridotites along a 40 mW/m^2 geotherm. The normative densities (Figure 10a) are compared to the isopycnic densities for a 200 km thick thermal boundary layer using an oceanic reference norma-

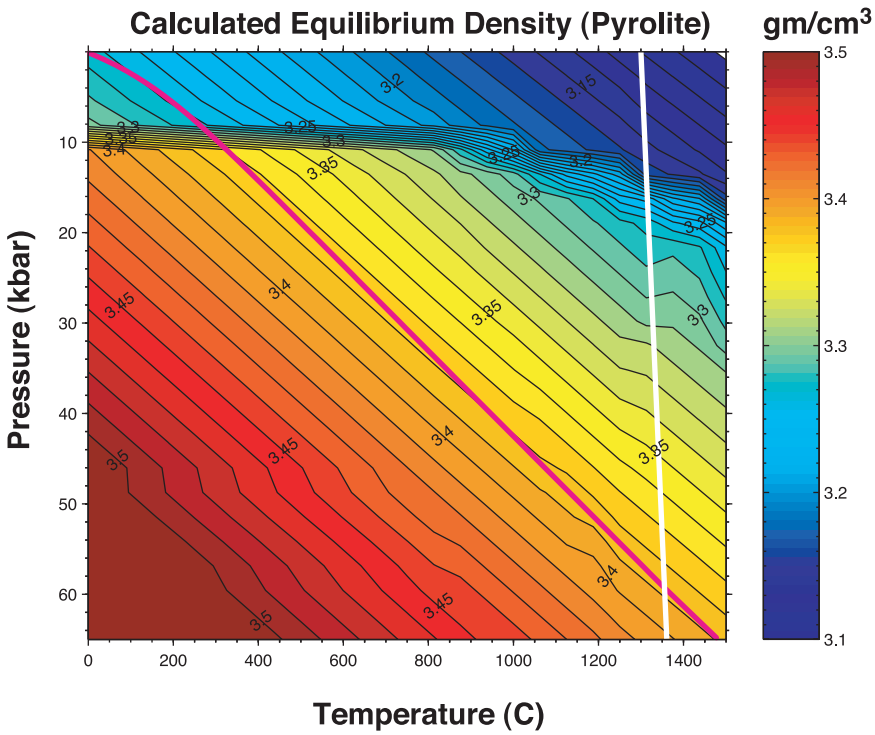

Figure 9. Contours of equilibrium density calculated using *Perplex* for pyrolite [*Ringwood*, 1966] from 0–65 kbar and 0–1500°C. The magenta line represents a 40 mW/m^2 conductive geotherm, and the white line illustrates an adiabat with a mantle potential temperature of 1300°C.

tive density of 3.4 gm/cm^3 [*Jordan*, 1988]. Since normative density is a linear function of Mg#, it can be inferred from Figure 10a that Mg# does not vary systematically with depth in the Kaapvaal low-temperature xenolith suite. This appears to be true in Archean cratons worldwide, with the exception of the Alakit kimberlite xenoliths in the Siberian craton [*Gaul et al.*, 2000]. The model equilibrium densities are shown relative to the *Perplex*-calculated density of pyrolite along an adiabat with a potential temperature of 1300°C (Figure 10b). The great majority of the xenolith samples have both a lower normative density and a lower equilibrium density at their pressures of equilibration than would be expected for an isopycnic condition.

[23] Pyrolite densities at each pressure along an adiabatic geotherm with a potential temperature of 1300°C (Figure 9) were subtracted from the mantle xenolith equilibrium densities at the corresponding pressures over the entire range of temperatures. This produced a value for the density difference, $\Delta\rho$, for each sample at any temperature and pressure relative to pyrolite at the same pressure along the 1300°C adiabat. Figure 11 illustrates $\Delta\rho$ for garnet peridotite xenolith PHN 4274 in Figure 8. Where $\Delta\rho$ is positive, samples are denser than the convecting mantle at a given pressure; where $\Delta\rho$ is negative, samples are buoyant with respect to the convecting mantle at the same depth.

[24] Values of $\Delta\rho$ for all the peridotites along a 40 mW/m^2 conductive geotherm (ρ sample on geotherm - ρ pyrolite on adiabat) are plotted as a function of pressure in Figure 12. For reference, a line for $\Delta\rho$ for pyrolite along a conductive geotherm is included. Rectangles illustrate the range of pressures for which Kaapvaal mantle peridotite xenoliths are neutrally buoyant compared to pyrolite along a 1300°C adiabat.

[25] Figure 13 compares equilibration pressures and the pressures at which equilibrium densities

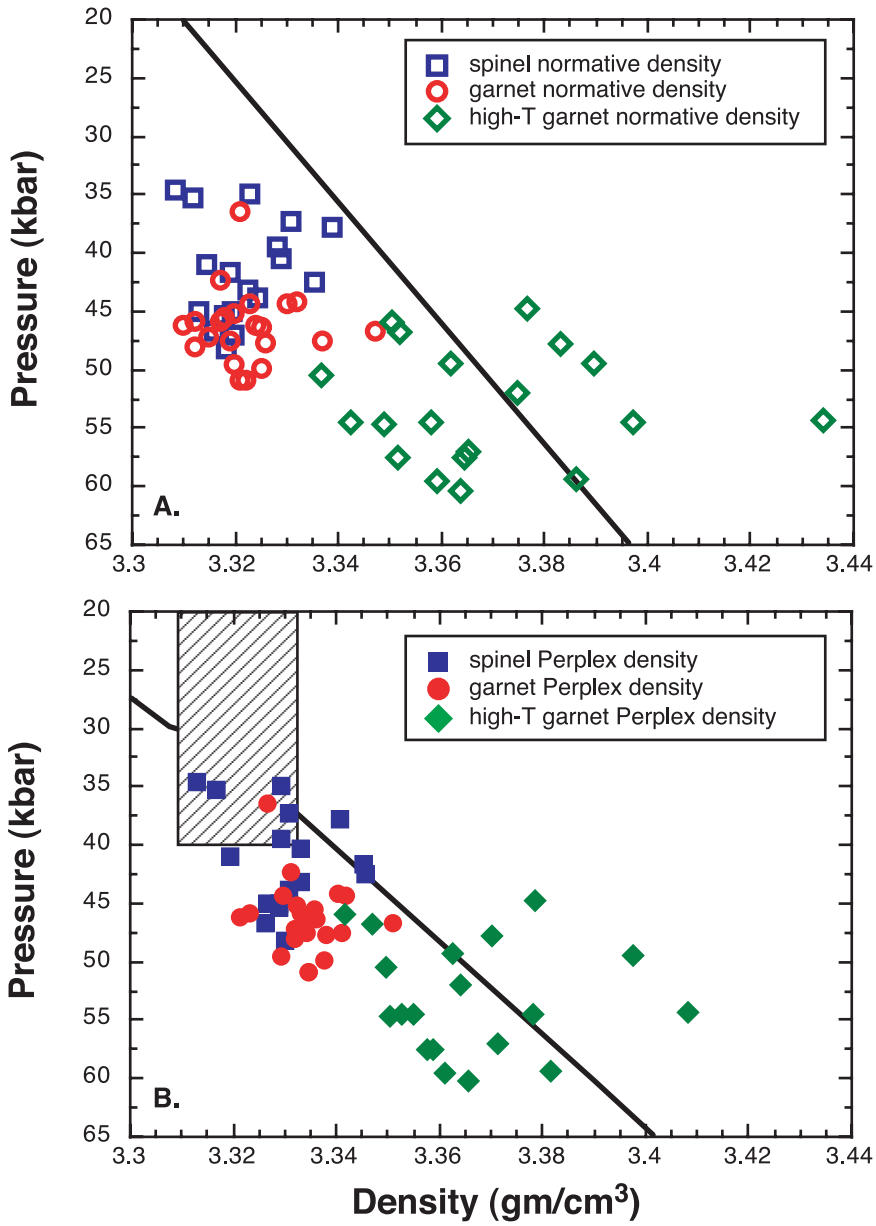

Figure 10. (a) Normative densities [*Jordan*, 1988] for the garnet and spinel peridotite xenoliths plotted at the equilibration pressures for each sample. Open blue squares are spinel peridotites, open red circles are low-temperature garnet-bearing peridotites, and open green diamonds are high-temperature garnet peridotites. The black line represents isopycnic densities for a thermal boundary layer thickness of 200 km (66.67 kbar) using a normative asthenospheric density of 3.4 gm/cm^3 [*Jordan*, 1988]. Most normative densities for the Kaapvaal mantle xenoliths are positively buoyant relative to the isopycnic line. Only a few high-temperature garnet peridotites have higher normative density compared to the convecting asthenosphere at the same depth. (b) Calculated equilibrium densities (*Perplex*) for the Kaapvaal spinel and garnet mantle peridotite suite along a 40 mW/m^2 conductive geotherm plotted at the pressures of equilibration for each sample. The majority of xenoliths have a lower density than the asthenospheric mantle (*Perplex*-calculated pyrolite density) along an adiabat with a potential temperature of 1300°C (black line). Gray, diagonally ruled rectangle shows the range of densities for hypothetical spinel peridotites in the uppermost mantle, as presented in Figure 14 and accompanying text.

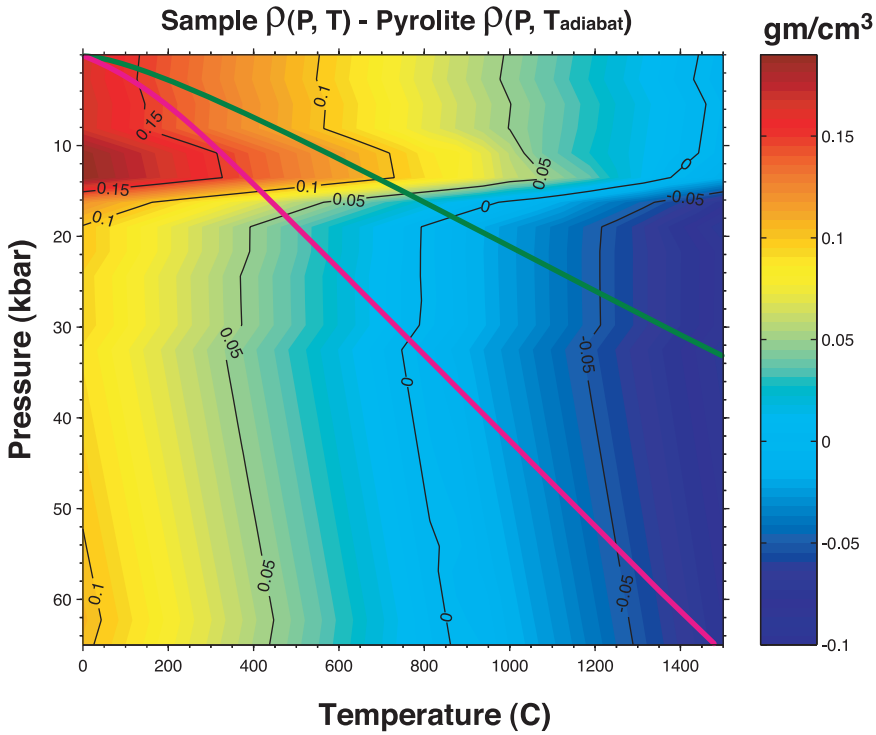

Figure 11. Difference between equilibrium densities for Kaapvaal garnet-bearing peridotite PHN 4274 (Figure 8) and pyrolite densities along an adiabat with a mantle potential temperature of 1300°C (Figure 9), where $\Delta\rho = \rho_{sample}$ (P, T) − $\rho_{pyrolite}$ (P, $T_{adiabat}$). Any geotherm can be selected within this grid to determine the density difference between the Kaapvaal peridotite and pyrolite along an adiabat. A 40 mW/m^2 conductive geotherm is shown in magenta, and a hypothetical conductive geotherm during craton formation, which intersects a 1500°C adiabat at 100 km, is shown in green. The point at which $\Delta\rho = 0$ along the conductive geotherm is the "crossover pressure," above which a peridotite with this bulk composition will become positively buoyant relative to pyrolite. Crossover pressures are much lower on a hotter "Archean" geotherm, compared to the 40 mW/m^2 geotherm.

on a conductive geotherm are neutrally buoyant relative to pyrolite on an adiabat ($\Delta\rho = 0$). Pressures of neutral buoyancy are systematically lower than pressures of equilibration.

4. Discussion

4.1. Thermobarometry and Phase Assemblages

[26] Thermobarometry of mantle peridotite xenoliths from Archean cratons such as the Kalahari, Slave, Siberia, and Superior cratons produces equilibration temperatures and pressures that lie along a conductive geotherm that intersects a mantle adiabat at about 200 km depth [e.g., *Finnerty and Boyd*, 1987; *Rudnick et al.*, 1998; *Rudnick and Nyblade*, 1999]. This result is similar to a 40 mW/m^2 conductive geotherm and to PT estimates for the low-temperature Kaapvaal xenoliths (Figure 4), suggesting that the conductively cooled cratonic thermal boundary layer beneath Kaapvaal was in a thermal steady state prior to the time the kimberlites were erupted. The ages of Kaapvaal kimberlites that host the xenoliths imply that a steady state geotherm in the ~200 km thick lithospheric mantle section beneath Kaapvaal must have been established earlier than 1200 Ma and been sustained until after 100 Ma [e.g., *Richardson*, 1986; *Smith et al.*, 1994].

[27] Along the 40 mW/m^2 conductive geotherm, the calculated equilibration temperatures of the spinel peridotites fall within the garnet peridotite stability field, yet these xenoliths do not contain garnet. Spinel is not stabilized to unusually high pressures by high Cr-contents; among Kaapvaal

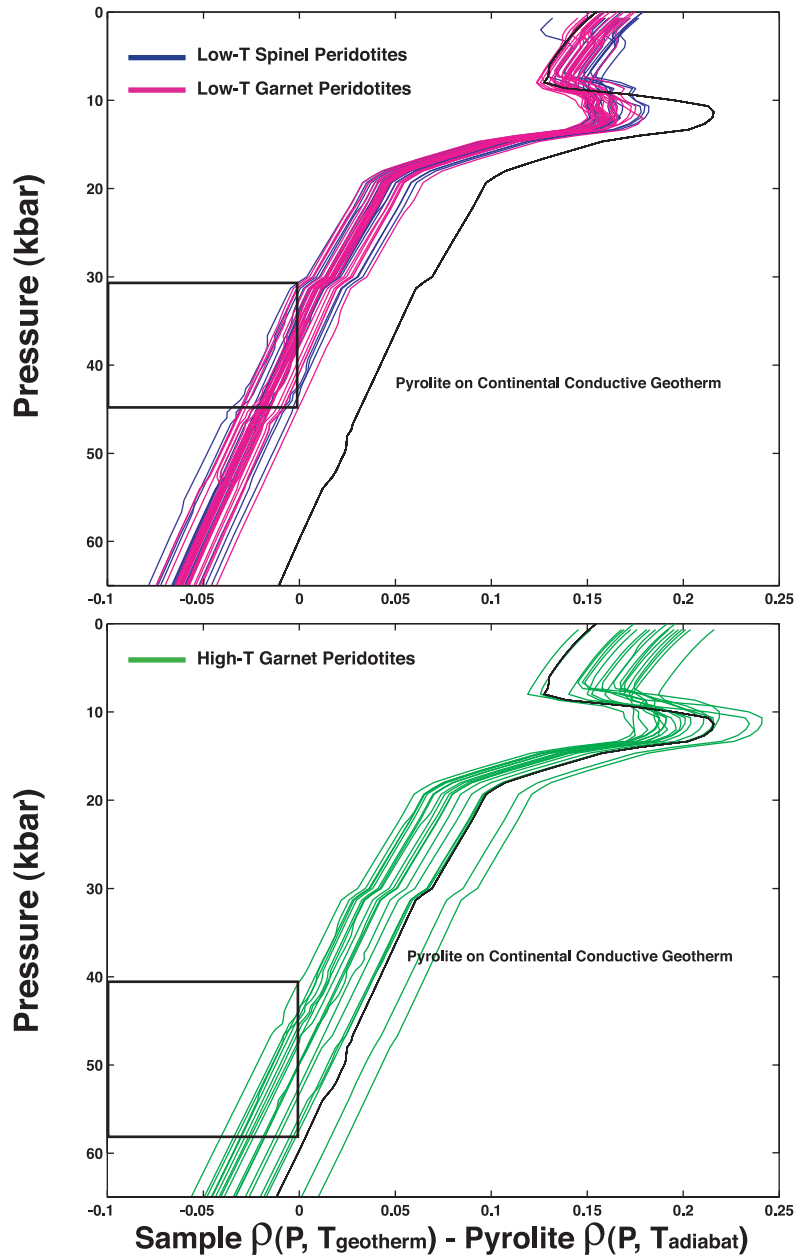

Figure 12. (top) Calculated $\Delta\rho$ for the suite of Kaapvaal spinel and low-temperature, garnet-bearing peridotites along a 40 mW/m^2 conductive geotherm (ρ sample on geotherm - ρ pyrolite on an adiabat at the same pressure and a mantle potential temperature of 1300°C), plotted against pressure. The spinel peridotites are in blue, and the garnet-bearing peridotites are in red. The solid black line represents $\Delta\rho$ for pyrolite on the conductive geotherm. The open black box indicates the range of pressures for which this suite of samples is neutrally buoyant relative to pyrolite on the adiabat. (bottom) Green lines illustrate $\Delta\rho$ for high-temperature Kaapvaal garnet peridotites. Note that the crossover pressures for the high-temperature garnet peridotites (open black box) are higher than those for the low-temperature peridotites, and that two samples are not positively buoyant relative to pyrolite on the adiabat at any pressure between 0 and 65 kbar.

xenoliths, spinel peridotites are not systematically more Cr-rich than garnet peridotites. However, there are several possible explanations for the absence of garnet in spinel peridotites that are consistent with available data. One viable hypothesis is that the equilibration pressures for the spinel peridotites inferred from their temperatures along a 40 mW/m^2 geotherm are incorrect. A hotter geo-

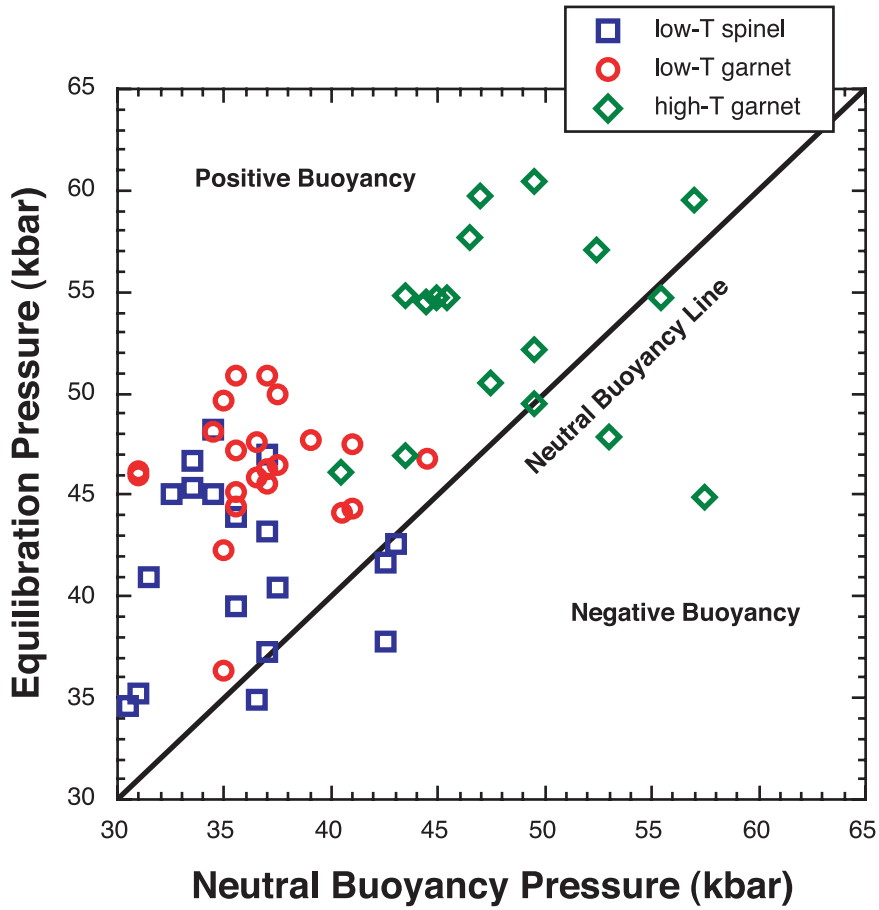

Figure 13. Comparison of sample equilibration pressure to the crossover pressure, at which a given sample becomes neutrally buoyant along a 40 mW/m^2 conductive geotherm relative to pyrolite on an adiabat with a mantle potential temperature of 1300°C. Most of the calculated equilibration pressures for the suite of analyzed Kaapvaal peridotites are higher than the pressure at which each sample would be neutrally buoyant. These samples are positively buoyant.

therm, as suggested by some of the garnet-bearing xenoliths, would result in lower projected equilibration pressures for the spinel-bearing xenoliths. However, inferred pressures would still be greater than 25 kbar, which is within the garnet lherzolite stability field at ~800°C, and inferred pressure/temperature conditions would still overlap with those of garnet peridotite xenoliths. A second possibility is that the spinel-bearing xenoliths were recently reheated, for example by a magmatic process, so that they do not record temperatures along the steady state conductive geotherm. In this case, their depths of equilibration are unknown and could be within the spinel lherzolite stability field. Third, Al/Cr exchange within phases, used to calculate the temperature, may be more rapid than garnet nucleation and growth; isobaric cooling into the garnet lherzolite stability field is recorded by the thermometer, but the phase assemblage is "stuck" at a higher temperature. And fourth, the closure temperature for the Al-Cr orthopyroxene/spinel exchange thermometer might have been high when the spinel peridotites initially cooled; in this case, the steady state temperature for the spinel peridotites is lower than we calculate using the Al-Cr thermometer.

[28] The program *Perplex* [*Connolly*, 1990] uses bulk rock compositions to determine the solid phase proportions and solid solution compositions at different pressures and temperatures by free energy minimization. From the predicted mineral phase assemblages at each pressure and temper-

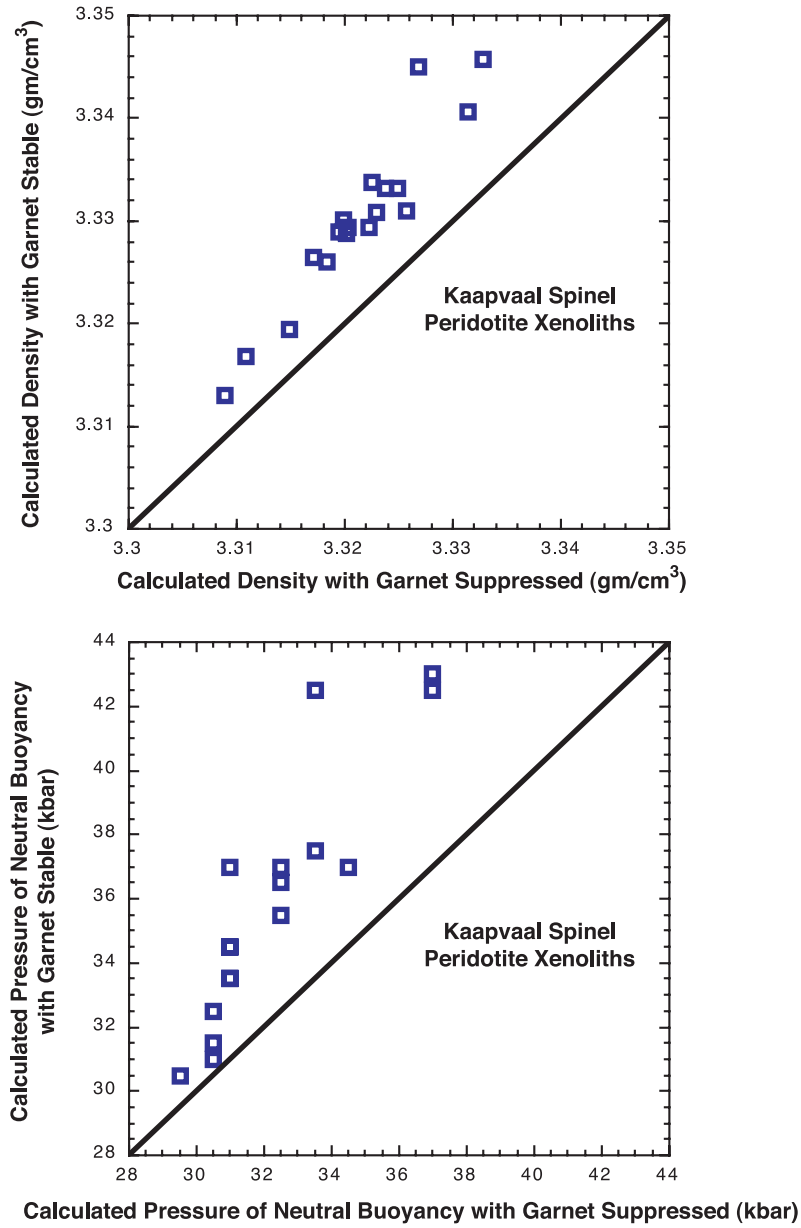

Figure 14. Calculated densities and pressures of neutral buoyancy for Kaapvaal spinel peridotite xenolith compositions. The top panel compares densities at the equilibration temperature and the corresponding pressure along a 40 mW/m^2 conductive geotherm, with and without garnet in the calculated phase assemblage. The bottom panel compares the crossover pressure at which each composition along a 40 mW/m^2 conductive geotherm becomes neutrally buoyant with respect to pyrolite on an adiabat with a potential temperature of 1300°C, again with and without garnet in the phase assemblage. Garnet-free densities for spinel peridotite xenoliths, calculated using *Perplex*, are also shown as a diagonally ruled rectangle in Figure 10b. Predicted garnet in the *Perplex* phase assemblages for the spinel peridotites leads to an overprediction of equilibrium densities, as seen in the top panel. The pressures at which the spinel peridotites become neutrally buoyant relative to pyrolite are shallower when garnet formation is suppressed in the *Perplex* calculations, as seen in the bottom panel.

ature, the density of the material can be calculated. As already discussed in the first two paragraphs of section 3.2, one of the main drawbacks to using *Perplex* for the Kaapvaal mantle peridotite xenoliths is that the model does not incorporate Cr_2O_3 into any phases. In natural assemblages, the presence of Cr-bearing spinel suppresses the onset of garnet formation during cooling or compression.

The end-member garnet-bearing phase assemblage is denser than the Cr-spinel end-member assemblage, so excess garnet in the Cr-free peridotite compositions used for *Perplex* might lead to an overestimate of density at a given pressure and temperature. In order to determine the magnitude of this effect, we ran test cases for the spinel xenolith compositions in which garnet formation was suppressed. The equilibrium densities of the garnet-free assemblages were lower than when garnet was allowed to form (Figure 14). These differences are less than 0.5% and are insignificant compared to the variation in density observed in the entire data set. However, we note that the pressures at which peridotites are neutrally buoyant relative to pyrolite are shallower for the garnet-free assemblages (Figure 14).

4.2. Positively Buoyant Cratonic Mantle Peridotites

[29] The bulk rock Mg#s combined with calculated equilibration pressures allow a comparison of the normative densities of the Kaapvaal low-temperature garnet and spinel peridotite xenoliths to isopycnic densities. As seen in Figure 10a, for all of the low-temperature peridotites and the majority of the high-temperature peridotites, the normative densities are lower than isopycnic densities for a 200 km thick thermal boundary layer. This implies that these mantle xenoliths have compositions that are positively buoyant along a conductive geotherm when compared to the adiabatically convecting mantle at the same depth. This supports the *Kelemen et al.* [1998] hypothesis that the cratonic upper mantle may be positively buoyant, rather than neutrally buoyant as suggested by *Jordan* [1988]. However, normative density estimates are open to question.

[30] For the garnet and spinel peridotite bulk rock compositions provided by F.R. Boyd, predicted equilibrium phase assemblages can be used to calculate equilibrium densities at a range of pressures and temperatures, as in the example in Figure 8. These densities can then be compared to those of pyrolite (Figure 9) along an adiabatic geotherm with a potential temperature of 1300°C (example in Figure 11).

[31] The difference between calculated equilibrium densities for all xenolith compositions on a 40 mW/m^2 conductive geotherm and pyrolite along an adiabat with a potential temperature of 1300°C has been plotted against pressure in Figure 12. All of the low-temperature peridotites and all but two of the high-temperature xenoliths have bulk rock compositions that will become neutrally buoyant relative to adiabatic pyrolite in the range of 0–65 kbar given sufficiently high pressure. Figure 13 demonstrates that, for the majority of these xenoliths, the pressure at which each sample equilibrated is greater than the pressure at which it would become neutrally buoyant relative to pyrolite on an adiabat. Thus, most of these peridotites are estimated to be positively buoyant relative to the convecting mantle at their respective equilibration pressures.

[32] These results agree with the *Griffin et al.* [1998, 1999] and *Poudjom Djomani et al.* [2001] studies of Kaapvaal mantle buoyancy. However, these authors emphasized that the entire craton might be positively buoyant, whereas we prefer the hypothesis that the craton is neutrally buoyant, because we are persuaded by the long-term retention of a thin but ancient sedimentary cover, and the result that topography in southern Africa may be dynamically supported [e.g., *Lithgow-Bertelloni and Gurnis*, 1997; *Lithgow-Bertelloni and Silver*, 1998].

[33] As the compositions of the Kaapvaal peridotites yield equilibration pressures no lower than 30 kbar, the composition, and therefore the buoyancy, of the upper part of the mantle thermal boundary layer is poorly known. Peridotite compositions analogous to the Kaapvaal garnet and spinel peridotite xenoliths would be neutrally or negatively buoyant at shallower pressures due to the lower temperatures along a cratonic geotherm. Therefore there could be a negatively buoyant layer of spinel peridotite between the base of the crust at about 40 km depth and about 75 km depth (see diagonally ruled area in Figure 10b). This might be sufficient to offset the positive buoyancy of compositionally similar, hotter peridotites at greater depth.

[34] The presence of high-density eclogite layers in the lower crust or upper mantle could also compensate for the positively buoyant spinel and garnet

peridotites, resulting in a neutrally buoyant thermal boundary layer. *Schulze* [1989] calculated 3–15% eclogite by volume from the Roberts Victor, Bobbejaan, and Zagadochnaya kimberlites in southern Africa and Siberia. This is sufficient to balance the positive buoyancy of depleted cratonic peridotite. For example, 93% Kaapvaal peridotite ($\rho \sim 3.335$ gm/cm^3) and 7% eclogite ($\rho \sim 3.600$ gm/cm^3) could be neutrally buoyant with respect to pyrolite on an adiabat ($\rho \sim 3.353$ gm/cm^3) at an average pressure of $\sim$ 45 kbar within the pressure range from 30 to 65 kbar (e.g., Figure 10b).

4.3. Effect of Hotter Archean Geotherm

[35] As cratons began to form, the thermal boundary layer would have been thinner than at present. If the thermal boundary layer were 100 km thick, rather than 200 km thick, the conductive geotherm would have been steeper. Also, the mantle potential temperature may have been higher in the Archean. As can be observed from the example in Figure 11, compositions of the Kaapvaal garnet and spinel peridotite xenoliths are neutrally or positively buoyant with respect to the convecting mantle at low pressures, provided the temperatures are high enough. Thus, peridotites with the composition of the Kaapvaal xenoliths would have been neutrally to positively buoyant at shallow depth when they originally began to accumulate. As the cratons thickened and the conductive geotherm relaxed through time, the peridotites toward the base of the thermal boundary layer remained positively or neutrally buoyant in comparison to the underlying convecting asthenospheric mantle, while those at cooler temperatures and shallower depths may have become neutrally or negatively buoyant.

5. Conclusions

[36] Thermobarometry of Kaapvaal garnet and spinel peridotites yields estimated equilibration pressures greater than 30 kbar for all samples, with some originating as deep as 60 kbar. The garnet peridotites fall along a conductive geotherm with a surface heat flux of $\sim$40 mW/m^2, or slightly higher, similar to that proposed for the continents by *Pollack and Chapman* [1977]. This geotherm intersects a mantle adiabat with a potential temperature of 1300°C at about 200 km depth.

[37] Using the relationship between whole rock Mg# and normative density described by *Jordan* [1988], the majority of the Kaapvaal xenoliths in a 200 km thick thermal boundary layer are estimated to be positively buoyant compared to the asthenosphere. Using bulk rock compositions of these xenoliths and calculations of the equilibrium subsolidus phase assemblage (*Perplex* [*Connolly*, 1990]), we calculated the densities of the xenolith compositions for a range of pressures and temperatures. As for the normative densities, calculated equilibrium densities for most Kaapvaal xenolith compositions are positively buoyant compared to pyrolite on an adiabat with a mantle potential temperature of 1300°C. At pressures less than their equilibration pressures, the xenolith compositions are negatively buoyant along a 40 mW/m^2 conductive geotherm. However, they would have been positively or neutrally buoyant at low pressure at high temperature during craton formation, given a thinner thermal boundary layer and/or higher mantle potential temperatures in the Archean.

[38] These results suggest that much of the depleted peridotite component of the cratonic upper mantle is positively buoyant with respect to the surrounding, convecting mantle. The absence of either uplift or substantial departures from isostasy suggests that the cratons as a whole are neutrally buoyant. Therefore some other component of the cratons, perhaps a shallow layer of dense spinel peridotite, eclogite layers within the mantle, or garnet granulites at the base of the crust, is negatively buoyant and offsets the positive buoyancy of the depleted peridotites (Figure 3). A region of positively buoyant peridotite near the base of the lithospheric mantle could help explain the long-term stability of continental cratons.

Acknowledgments

[39] We would like to thank F.R. Boyd for generously providing us with Kaapvaal peridotite xenolith bulk rock and mineral composition data. We also thank Cin-Ty Lee for his assistance in adding to the mineral composition data, Jamie

Connolly for his help with the thermodynamic calculations, Claude Jaupart for encouragement, and Neal Driscoll for his advice on isostasy. Cin-Ty Lee, Bill Griffin, and Roberta Rudnick provided their insightful and helpful reviews. This research was supported by NSF grants EAR-9814632 and EAR-9910899 (P. B. Kelemen), and EAR-0087706 (M. Jull and P. B. Kelemen).

References

Bass, J. D., Elasticity of minerals, glasses, and melts, in *Mineral Physics and Crystallography: A Handbook of Physical Constants*, edited by T. J. Ahrens, pp. 45–63, AGU, Washington, D. C., 1995.

Bernstein, S., P. B. Kelemen, and C. K. Brooks, Depleted spinel harzburgite xenoliths in Tertiary dykes from East Greenland: Restites from high degree melting, *Earth Planet. Sci. Lett.*, *154*, 221–235, 1998.

Bird, P., Continental delamination and the Colorado plateau, *J. Geophys. Res.*, *84*, 7561–7571, 1979.

Boyd, F. R., Compositional distinction between oceanic and cratonic lithosphere, *Earth Planet. Sci. Lett.*, *96*, 15–26, 1989.

Boyd, F. R., and R. H. McCallister, Densities of fertile and sterile garnet peridotites, *Geophys. Res. Lett.*, *3*, 509–512, 1976.

Boyd, F. R., N. P. Pokhilenko, D. G. Pearson, S. A. Mertzman, N. V. Sobolev, and L. W. Finger, Composition of the Siberian cratonic mantle: Evidence from Udachnaya peridotite xenoliths, *Contrib. Mineral. Petrol.*, *128*, 228–246, 1997.

Boyd, F. R., D. G. Pearson, and S. A. Mertzman, Spinel-facies peridotites from the Kaapvaal Root, in *Proceedings of the VIIth International Kimberlite Conference*, vol. 1, edited by J. J. Gurney et al., pp. 40–48, Red Roof Design, Cape Town, South Africa, 1999.

Brey, G. P., and T. Kohler, Geothermobarometry in four-phase lherzolites, II, New thermobarometers, and practical assessment of existing thermobarometers, *J. Petrol.*, *31*, 1353–1378, 1990.

Connolly, J. A. D., Multivariable phase diagrams: An algorithm based on generalized thermodynamics, *Am. J. Sci.*, *290*, 666–718, 1990.

Dziewonski, A. M., Mapping the lower mantle: Determination of lateral heterogeneity in P velocity up to degree and order 6, *J. Geophys. Res.*, *89*, 5929–5952, 1984.

Eggler, D. H., M. E. McCallum, and M. B. Kirkley, Kimberlite-transported nodules from Colorado-Wyoming: A record of enrichment of shallow portions of an infertile lithosphere, *Spec. Pap. Geol. Soc. Am.*, *215*, 77–90, 1987.

Finnerty, A. A., and F. R. Boyd, Thermobarometry for garnet peridotites: Basis for the determination of thermal and compositional structure of the upper mantle, in *Mantle Xenoliths*, edited by P. H. Nixon, pp. 381–402, Wiley-Interscience, New York, 1987.

Forsyth, D. W., Subsurface loading and estimate of flexural rigidity of continental lithosphere, *J. Geophys. Res.*, *90*, 12,623–12,632, 1985.

Gaul, O. F., W. L. Griffin, S. Y. O'Reilly, and N. J. Pearson, Mapping olivine composition in the lithospheric mantle, *Earth Planet. Sci. Lett.*, *182*, 223–235, 2000.

Goes, S., and S. van der Lee, Thermal structure of the North American uppermost mantle inferred from seismic tomography, *J. Geophys. Res.*, *107*(B3), 2050, doi:10.1029/2000JB000049, 2002.

Grand, S. P., R. D. van der Hilst, and S. Widiyantoro, Global seismic tomography: A snapshot of convection in the Earth, *GSA Today*, *7*, 1–7, 1997.

Green, D. H., and R. C. Lieberman, Phase equilibria and elastic properties of a pyrolite model for the oceanic upper mantle, *Tectonophysics*, *32*, 61–92, 1976.

Griffin, W. L., S. Y. O'Reilly, C. G. Ryan, O. Gaul, and D. A. Ionov, Secular variation in the composition of subcontinental lithospheric mantle: Geophysical and geodynamic implications, in *Structure and Evolution of the Australian Continent*, *Geodyn. Ser.*, vol. 26, edited by J. Braun et al., pp. 1–25, AGU, Washington, D. C., 1998.

Griffin, W. L., S. Y. O'Reilly, and C. G. Ryan, The composition and origin of subcontinental lithospheric mantle, in *Mantle Petrology: Field Observations and High-Pressure Experimentation, A Tribute to Francis R. (Joe) Boyd*, edited by Y. Fei, C. M. Bertka, and B. O. Mysen, *Spec. Publ. Geochem. Soc.*, *6*, 13–45, 1999.

Hacker, B. R., Eclogite formation and the rheology, buoyancy, seismicity and H_2O content of oceanic crust, in *Subduction Top to Bottom*, *Geophys. Monogr. Ser.*, vol. 96, edited by G. E. Bebout et al., pp. 337–346, AGU, Washington, D. C., 1996.

Hager, B. H., R. W. Clayton, M. A. Richards, R. P. Comer, and A. M. Dziewonski, Lower mantle heterogeneity, dynamic topography, and the geoid, *Nature*, *313*, 541–545, 1985.

Haxby, W. F., and D. L. Turcotte, On isostatic geoid anomalies, *J. Geophys. Res.*, *83*, 5473–5478, 1978.

Holland, T. J. B., and R. Powell, An internally consistent thermodynamic data set for phases of petrological interest, *J. Metamorph. Geol.*, *16*, 309–343, 1998.

Houseman, G. A., D. P. McKenzie, and P. Molnar, Convective instability of a thickening boundary layer and its relevance for the thermal evolution of continental convergent belts, *J. Geophys. Res.*, *86*, 6115–6132, 1981.

Jordan, T. H., The continental tectosphere, *Rev. Geophys.*, *13*, 1–12, 1975a.

Jordan, T. H., Lateral heterogeneity and mantle dynamics, *Nature*, *257*, 745–750, 1975b.

Jordan, T. H., Mineralogies, densities, and seismic velocities of garnet lherzolites and their geophysical implications, in *The Mantle Sample: Inclusions in Kimberlites and Other Volcanics*, edited by F. R. Boyd and H. O. A. Meyer, pp. 1–14, AGU, Washington, D. C., 1979.

Jordan, T. H., Structure and formation of the continental tectosphere, *J. Petrol. (Special Lithosphere Issue)*, 11–37, 1988.

Karner, G. D., and A. B. Watts, Gravity anomalies and flexure of the lithosphere at mountain ranges, *J. Geophys. Res.*, *88*, 10,449–10,477, 1983.

Karner, G. D., M. S. Steckler, and J. A. Thorne, Long-term thermo-mechanical properties of the continental lithosphere, *Nature*, *304*, 250–253, 1983.

Kelemen, P. B., S. R. Hart, and S. Bernstein, Silica entrenchment in the continental upper mantle via melt/rock reaction, *Earth Planet. Sci. Lett.*, *164*, 387–406, 1998.

Kopylova, M. G., J. K. Russell, and H. Cookenboo, Upper-mantle stratigraphy of the Slave craton, Canada: Insights into a new kimberlite province, *Geology*, *26*, 315–318, 1998.

Kopylova, M. G., J. K. Russell, and H. Cookenboo, Petrology of peridotite and pyroxenite xenoliths from the Jericho kimberlite: Implications for the thermal state of the mantle beneath the Slave Craton, Northern Canada, *J. Petrol.*, *40*, 79–104, 1999.

Kusznir, N., and G. Karner, Dependence of the flexural rigidity of the continental lithosphere on rheology and temperature, *Nature*, *316*, 138–142, 1985.

Larsen, J. G., Mantle-driven dunite and lherzolite nodules from Ubekendt Ejland, west Greenland Tertiary province, *Mineral. Mag.*, *46*, 329–336, 1982.

Lee, C.-T., and R. L. Rudnick, Compositionally stratified cratonic lithosphere: Petrology and geochemistry of peridotite xenoliths from the Labait Volcano, Tanzania, in *Proceedings of the VIIth International Kimberlite Conference*, edited by J. J. Gurney et al., pp. 503–521, Red Roof Design, Cape Town, South Africa, 1999.

Lee, C.-T., Q. Yin, R. L. Rudnick, and S. B. Jacobsen, Preservation of ancient and fertile lithospheric mantle beneath the southwestern United States, *Nature*, *411*, 69–73, 2001.

Li, X. D., and B. Romanowicz, Global shear-velocity model developed using nonlinear asymptotic coupling theory, *J. Geophys. Res.*, *101*, 22,245–22,272, 1996.

Lithgow-Bertelloni, C., and M. Gurnis, Cenozoic subsidence and uplift of continents from time-varying dynamic topography, *Geology*, *25*, 735–738, 1997.

Lithgow-Bertelloni, C., and P. G. Silver, Dynamic topography, plate driving forces and the African superswell, *Nature*, *395*, 269–272, 1998.

Lowry, A. R., and R. B. Smith, Flexural rigidity of the Basin and Range-Colorado Plateau-Rocky Mountain transition from coherence analysis of gravity and topography, *J. Geophys. Res.*, *99*, 20,123–20,140, 1994.

Menzies, M. A., Geochemistry: Effects of small volume melts, *Nature*, *343*, 312–313, 1990.

Mitchell, R. H., Ultramafic xenoliths from the Elwin Bay kimberlite: The first Canadian paleogeotherm, *Can. J. Earth Sci.*, *14*, 1202–1210, 1977.

Mitchell, R. H., Garnet lherzolites from Somerset Island, Canada, and aspects of the nature of perturbed geotherms, *Contrib. Mineral. Petrol.*, *67*, 341–347, 1978.

Nyblade, A. A., and S. W. Robinson, The African superswell, *Geophys. Res. Lett.*, *21*, 765–768, 1994.

O'Hara, M. J., Is there an Icelandic mantle plume?, *Nature*, *253*, 708–710, 1975.

O'Reilly, S. Y., W. L. Griffin, Y. H. Poudjom Djomani, and P. Morgan, Are lithospheres forever? Tracking changes in subcontinental lithosperic mantle through time, *GSA Today*, *11*, 4–9, 2001.

Oxburgh, E. R., and E. M. Parmentier, Thermal processes in the formation of continental lithosphere, *Philos. Trans. R. Soc. London, Ser. A*, *288*, 415–429, 1978.

Parsons, B., and D. McKenzie, Mantle convection and the thermal structure of the plates, *J. Geophys. Res.*, *83*, 4485–4496, 1978.

Parsons, B., and F. M. Richter, A relation between the driving force and geoid anomaly associated with mid-ocean ridges, *Earth Planet. Sci. Lett.*, *51*, 445–450, 1980.

Parsons, B., and J. G. Sclater, A analysis of the variation of ocean bathymetry and heat flow with age, *J. Geophys. Res.*, *82*, 803–827, 1977.

Pollack, H. N., and D. S. Chapman, On the regional variation of heat flow, geotherms, and lithospheric thickness, *Tectonophysics*, *38*, 279–296, 1977.

Poudjom Djomani, Y. H., J. M. Nnange, M. Diament, C. J. Ebinger, and J. D. Fairhead, Effective elastic thickness and crustal thickness variations in West-Central Africa inferred from gravity data, *J. Geophys. Res.*, *100*, 22,047–22,070, 1995.

Poudjom Djomani, Y. H., J. D. Fairhead, and W. L. Griffin, The flexural rigidity of Fennoscandia: Reflection of the tectonothermal age of the lithospheric mantle, *Earth Planet. Sci. Lett.*, *174*, 139–154, 1999.

Poudjom Djomani, Y. H., S. Y. O'Reilly, W. L. Griffin, and P. Morgan, The density structure of subcontinental lithosphere through time, *Earth Planet. Sci. Lett.*, *184*, 605–621, 2001.

Poupinet, G., and B. de Voogd, Some consequences of the differences in seismic properties in old and young continental plates for isostatic compensation, *Earth Planet. Sci. Lett.*, *56*, 278–286, 1981.

Richards, M. A., and B. H. Hager, Geoid anomalies in a dynamic earth, *J. Geophys. Res.*, *89*, 5987–6002, 1984.

Richardson, S. H., Latter-day origin of diamonds of eclogitic paragenesis, *Nature*, *322*, 623–626, 1986.

Ringwood, A. E., Mineralogy of the mantle, in *Advances in Earth Science: International Conference on the Earth Sciences*, edited by P. M. Hurley, pp. 357–399, MIT Press, Cambridge, Mass., 1966.

Rudnick, R. L., and A. A. Nyblade, The thickness and heat production of Archean lithosphere: Constraints from xenolith thermobarometry and surface heat flow, in *Mantle Petrology: Field Observations and High-Pressure Experimentation, A Tribute to Francis R. (Joe) Boyd*, edited by Y. Fei, C. M. Bertka, and B. O. Mysen, *Spec. Publ. Geochem. Soc.*, *6*, 3–12, 1999.

Rudnick, R. L., W. F. McDonough, and R. J. O'Connell, Thermal structure, thickness and composition of continental lithosphere, in *Geochemical Earth Reference Model (GERM)*, edited by F. Albarede et al., *Chem. Geol.*, *145*, 395–411, 1998.

Ryan, C. G., W. L. Griffin, and N. J. Pearson, Garnet geotherms: Pressure-temperature data from Cr-pyrope garnet xenocrysts in volcanic rocks, *J. Geophys. Res.*, *101*, 5611–5625, 1996.

Schulze, D. J., Constraints on the abundance of eclogite in the upper mantle, *J. Geophys. Res.*, *94*, 4205–4212, 1989.

Smith, C. B., T. C. Clark, E. S. Barton, and J. W. Bristow, Emplacement ages of kimberlite occurrences in the Prieska region, southwest border of the Kaapvaal Craton, South Africa, *Chem. Geol.*, *113*, 149–169, 1994.

Su, W.-J., R. L. Woodward, and A. M. Dziewonski, Degree 12 model of shear velocity heterogeneity in the mantle, *J. Geophys. Res.*, *99*, 6945–6980, 1994.

van der Hilst, R., S. Widiyantoro, and R. Engdahl, Evidence for deep mantle circulation from global tomography, *Nature*, *386*, 578–584, 1997.

Witt-Eickschen, G., and H. A. Seck, Solubility of Ca and Al in orthopyroxene from spinel peridotite: An improved version of an empirical geothermometer, *Contrib. Mineral. Petrol.*, *106*, 431–439, 1991.